Doctoral Thesis

Title: Formation of the endoplasmic reticulum-associated compartments by a Pma1 mutant and its physiological benefit in yeast cells

(酵母細胞における Pma1 変異体による小胞体関連コンパートメントの形成とその生理学的意義)

MAI CHI THANH

Nara Institute of Science and Technology

Division of Biological Sciences

Applied Stress Microbiology Laboratory

(Assoc. Prof. Yukio Kimata)

2021/01/18

Graduate School of Science and Technology Doctoral Thesis Abstract

Laboratory name (Supervisor)	Laboratory of Applied Stress Microbiology Laboratory (Assoc. Prof. KIMATA Yukio)		
Student ID	1821428	Submission date	2021/01/18 (yyyy/mm/dd)
Name (surname)(given name)	Mai Chi Thanh		
Title	Formation of the endoplasmic reticulum-associated compartments by a Pma1 mutant and its physiological benefit in yeast cells		

Abstract

It is commonly accepted that improper or insufficient folding of proteins is problematic for cells, not only because unfolded or misfolded proteins cannot exert proper functions, but also because they are hazardous. Unfolded proteins accumulated in cells interact with other functional proteins, which are then damaged. Unfolded proteins often form large aggregates, which can be a hallmark of a situation in which cells abundantly contain unfolded proteins. Therefore, in canonical understandings, protein aggregation *per se* is bad for cells, leading to various human diseases including Alzheimer's disease. On the other hand, it is also possible that the most hazardous status is not protein aggregates but aggregate-prone unfolded proteins that is not aggregated yet and is dispersed.

In eukaryotic cells, transmembrane proteins and secretory proteins are synthesized and folded in the endoplasmic reticulum (ER). Properly folded proteins are transported from the ER to their final destinations in which they work. On the other hand, when being misfolded or unfolded, proteins are retained in the ER and occasionally cause ER stress. Under ER stress conditions, an ER located transmembrane protein, Inositol-requiring enzyme 1 (Ire1), is activated to trigger a series of protective events that are collectively called the unfolded protein response (UPR). In yeast *Saccharomyces cerevisiae* cells, the activation of Ire1 leads to increment of the cellular abundance of Hac1, resulting in the transcriptional induction of various proteins including ER-located molecular chaperones and factors for clearance of unfolded proteins accumulated in the ER.

In yeast cells, some aberrant multimembrane-spanning proteins are not transported to the cell surface but form and are accumulated in ER-derived sub-compartments, known as the ER-associated compartments (ERACs). The ERACs are the place where the ER membrane changes its shape and is stacked. When ERAC-forming proteins are tagged with a fluorescent protein, they are observed as puncta being linked to the ER under the fluorescence microscopy.

Some properties of the yeast ERACs have been uncovered by using some model ERAC-forming proteins such as mutated Ste6 or the heterogenously expressed mammalian cystic fibrosis transmembrane conductance regulator (CFTR). According to a previous report by others, the COPII-forming machineries and the Hsp40-family chaperones assist the ERAC formation. While this observation implies that cells positively produce the ERACs, it has not been unclear if the ERAC formation is actually beneficial for yeast cells.

Here I show that a mutant form of the cell surface protein Pma1, namely Pma1-2308, was accumulated in the ERACs, as well as CFTR, in yeast cells. Pma1-2308 and CFTR were located on the same ERACs, suggesting that these two proteins form the ERACs through the same mechanism. However, unlike other ERAC-forming proteins including CFTR, Pma1-2308 evidently triggered the UPR, probably because it is stable and thus is accumulated in cells more abundantly than other ERAC-forming proteins. In agreement with this observation, growth retardation caused by cellular expression of Pma1-2308 was aggravated by the *ire1*-knock-out mutation.

4-phenyl butyric acid (4-PBA) is a chemical chaperone that prevents protein aggregation and suppresses the UPR of mammalian and yeast cells when added into the culturing media. Through an examination to determine the best working concentration of 4-PBA, I noticed that it should be added into yeast culture at a lower concentration than previously reported (1 mM versus 5 mM), because at high concentrations, it exhibited an undesired side effect, namely degradation of Ire1.

The UPR induced by treatment of yeast cells with a canonical ER-stressing reagent tunicamycin was suppressed by addition of 1-mM 4-PBA into the culturing medium. 4-PBA that was added into the culture at this concentration compromised the ERAC formation of Pma1-2308 and CFTR, suggesting that 4-PBA actually exerts a chaperone-like function in yeast cells. Intriguingly, in contrast to the case of the tunicamycin exposure, ER stress that was induced by Pma1-2308 was aggravated by 4-PBA. 4-PBA also increased the cell death caused by Pma1-2308.

I assume that this observation demonstrates a beneficial aspect of ERACs, and thus propose that the ERACs are formed through aggregation of aberrant transmembrane proteins and work as the accumulation sites of multiple ERAC-forming proteins for their sequestration.

Table of contents

I. INTRODUCTION

The endoplasmic reticulum (ER) of eukaryotic cells is a membrane-bound organelle where more than half of cellular proteins, such as transmembrane proteins and secretory proteins, are folded and modified. Only correctly folded and modified proteins are carried out from the ER and are transported to the Golgi apparatus, in which they are sorted for further transportation to the plasma membrane or another organelle where they work (Araki and Nagata, 2011). In other words, folding and modification of the ER client proteins is highly important for their appropriate function.

Proteins that are not correctly folded in the ER cannot reach their final destination and may cause cellular damage. The cystic fibrosis transmembrane conductance regulator (CFTR) of animals is a typical example. Wild-type CFTR forms a chloride channel which works on the plasma membrane of epithelia cells (Sheppard and Welsh, 1999). Since it is hard to be folded, only one-fifth of the CFTR molecules are folded properly even without mutations, and the residual misfolded species retain in the ER. Besides, some mutations of CFTR, including ΔF508 CFTR, promote its misfolding and cause an inherited disease called cystic fibrosis (Bobadilla et al., 2002; Riordan, 1999)

Moreover, when cells are chemically or pharmacologically stressed, protein folding and modification in the ER are often disrupted, leading to production of unfolded or misfolded proteins, which are accumulated in the ER. Such chemicals include dithiothreitol (DTT) and tunicamycin. DTT is a disulfide bond-reducing agent and causes unfolding of ER-client proteins through disturbing their disulfide-bond formation. Tunicamycin is an antibiotic that inhibits N-glycosylation of ER-client proteins.

Aberrant situations in which protein folding in the ER is impaired are collectively called ER stress. To ascertain that the protein folding process in the ER works properly, and to deal with ER stress, cells have various quality control systems. While they are carried commonly in eukaryotic species, their molecular mechanisms are frequently uncovered through studies in which budding yeast *Saccharomyces cerevisiae* (hereafter called yeast for short) was employed as a model organism.

The most prominent example of the quality control system is the unfolded protein response (UPR), which is the transcriptome change in response to ER stress. In yeast, an ER-located type-I transmembrane protein named Inositol-requiring enzyme 1 (Ire1) plays a central role in initiating the UPR (Mori, 2009;

Ron and Walter, 2007). Ire1 is conserved among eukaryote from yeast to human. The luminal domain of Ire1 senses unfolded peptides accumulated in the ER. On the other hand, the cytosolic domain, which carries both kinase and endoribonuclease (RNase) motives, is responsible for transferring the ER-stress signal to the downstream UPR signaling pathway (Mori et al., 1993; Shamu and Walter, 1996).

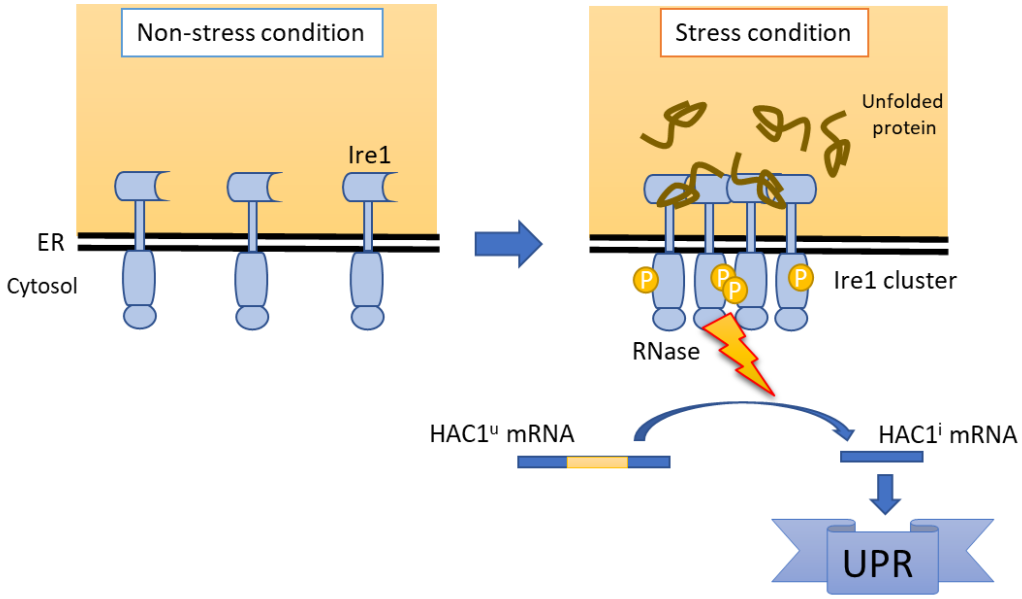

Figure 1. The Ire1-dependent UPR pathway in yeast cells: Under ER-stress conditions, Ire1molecules form homo-oligomers and promote auto-phosphorylation. The RNase activity of the Ire1 cytosolic domain then prompts the splicing of the *HAC1* mRNA to produce Hac1 protein, which is a transcription factor to induce the UPR.

The ER-luminal domain of Ire1 forms a groove-like structure which can capture unfolded proteins (Credle et al., 2005; Karagöz et al., 2017). Ire1 molecules bound to ER-accumulated unfolded proteins are self-associated to form high-order homo-oligomer (Gardner and Walter, 2011; Kimata et al., 2007). Moreover, in this stage, the Ire1 molecules promote trans-autophosphorylation, in which they phosphorylate each other in the oligomer (Shamu and Walter, 1996). These processes allow Ire1 to act as a potent RNase, which prompts the splicing of an mRNA named *HAC1* in yeast (or XBP1 in mammal). The spliced and mature *HAC1* mRNA then is translated to the Hac1 protein, which is a transcription factor to facilitate the UPR (Cox and Walter, 1996; Lee et al., 2008). In yeast, genes which induced by the UPR include those encoding ER-located molecular chaperones and factors for the clearance of unfolded proteins accumulated in the ER.

Degradation of misfolded or unfolded proteins stuck inside the ER is another intriguing process to cope with ER stress, and is performed in two different cellular machineries, namely proteasomes and lysosomes.

The proteasome is a cylindrical protein complex that forms an inner chamber core. Substrate proteins are perfectly unfolded, and are passed into the chamber from one end of the complex. Protease subunits contained in the chamber digest substrate proteins into short peptides, which will be released from another end of the complex (Tanaka, 2009). The most well-known pathway to direct ER-locate misfolded proteins to the proteasome is called ER-associate degradation (ERAD). For the ERAD, certain ER-located E3 ligase complexes mark substrate proteins by attaching ubiquitin to them, and translocates them from the ER lumen into the cytosol. This cellular process is thus named as retrotransport. In the cytosol, the ubiquitinated substrate proteins are brought to and digested by the proteasome (Thibaudeau and Smith, 2019). In yeast, Hdr1 and Doa10 are two major E3 ligases that work for the ERAD pathway (Zattas and Hochstrasser, 2015).

The ERAD, however, is limited by the size and conformation of substrate proteins. For instance, highly aggregated proteins, which are hard to be unfolded, are unable to be retrotranspoterd or to enter the proteasome chamber (Bustamante et al., 2018).

On the other hand, the lysosome can digest macromolecules including large-size proteins that are fully-folded or aggregated. The lysosome is a membrane-bound organelle, which carries many hydrolase enzymes (Ciechanover, 2005). By using proton pumps on its membrane, the lysosome lumen maintains acidic condition (pH 4.5-5), which is the best for the hydrolase enzymes to work. Although having similar functions as the mammalian lysosomes, the vacuoles in yeast or plant take a larger portion of volume in the cell, and has some other roles such as nutrition storage and hydrostatic pressure regulation (Lousa and Denecke, 2016).

Proteins or aged organelles are targeted to the lysosome through the autophagy pathway, which is regulated by the autophagy-related (ATG) proteins (Klionsky et al., 2003). Autophagy is started through surrounding of cargo substrates by membranes, resulting in formation of the autophagosome. The autophagosome is then fused with the lysosome, and the cargo substrates are degraded by the lysosomal hydrolase enzymes.

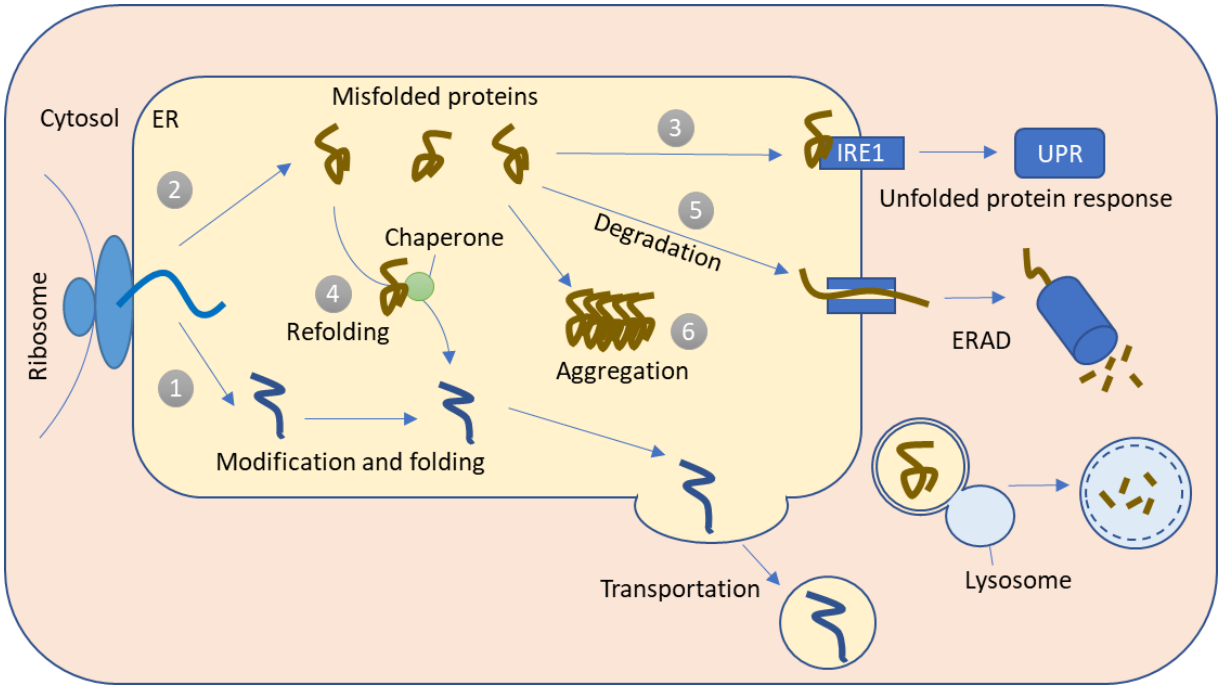

Figure 2. Fates of proteins in the ER. The ER is the place where proteins are synthesized and folded. If proteins are folded correctly, they are transported to their final destination (1). Misfolded proteins are retained in the ER (2) and trigger the unfolded protein response (UPR) (3). The UPR assist cells to handle misfolded proteins through inducing various ER proteins including molecular chaperones, which facilitate protein folding (4), or promoting misfolded-protein degradation (5). Misfolded proteins are also aggregated (6) when neither refolded nor degraded.

Abnormal proteins that fail to be degraded can be accumulated and/or aggregated. For instance, in mammalian cells, Russell bodies are formed through accumulation of misfolded immunoglobulins in the ER (Valetti et al., 1991). Moreover, in mammalian cells, ER stress is reported to form subcompartments of the ER, namely the ER-derived quality control compartment (ERQC), which contain misfolded proteins and some factors working for the quality control systems (Kondratyev et al., 2007).

Also in the case of yeast, a number of reports argue for focal formation of misfolded proteins. For instance, cytosolic misfolded proteins exhibit punctate distribution, namely the Q bodies, on the ER membrane (Escusa-Toret et al., 2013). As initially reported by Huyer (2004), it is also likely that misfolded membrane proteins are not transported to cell surface but are accumulated in proliferated subcompartments of the ER, which are named as the ER-associated compartments (ERACs). Under electron microscopy, the ERACs are observed as highly stacked ER (Huyer et al., 2004). Yeast endogenous transmembrane proteins such as Ste6 form the ERACs when carrying mutations. Heterologously expressed mammalian wild-type CFTR also forms and is accumulated in the ERACs even when not

carrying mutations. Under fluorescent microscopy, fluorescence-marked ERAC-forming proteins show punctate distribution on the ER (Fua and Sztula, 2009; Huyer et al., 2004).

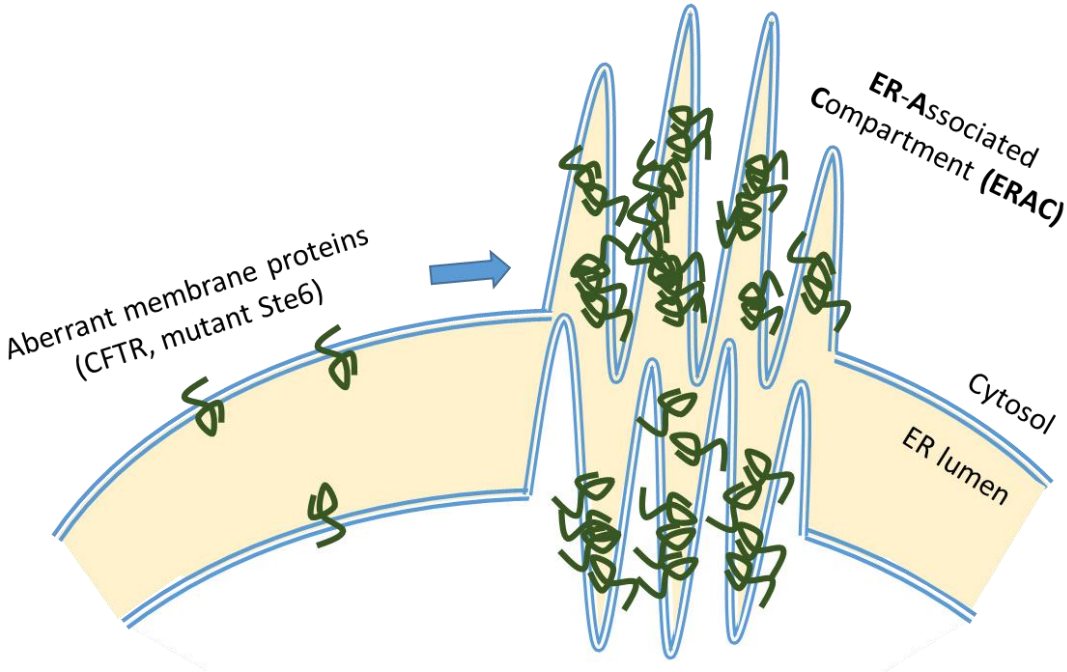

Figure 3. The ERACs in yeast cells: Some aberrant transmembrane proteins such as CFTR or mutant Ste6 form and are accumulated in an ER sub-compartments named as the ERACs.

It is possible that cells actively and positively form the ERACs when producing ER-forming proteins. In other words, the ERAC formation is a part of the ER quality control system. This is because, according to Kakoi et al. (2013), the COPII machinery and cytosolic Hsp40 family proteins act for the ERAC formation. This role of the COPII machinery is independent of the COPII function for the vesicular trafficking from ER to Golgi (Kakoi et al., 2013). In this context, the ERAC formation may be beneficial for cells, though no evidence has been provided for this idea. Moreover, it is also not clear how proteins are selected as the ERAC-forming proteins and whether different ERAC-forming proteins are located in the same ERACs.

For better understanding of properties of the ERACs, in the present study, we employed a mutant form of yeast plasma-membrane protein named Pma1 as a model substrate. Pma1 is 100 kilodaltons in size and belongs to the P-type ATPase transporters family. When carrying no mutations, this protein is delivered to the plasma membrane through the secretory pathway after being synthesized on the ER membrane. Pma1, which carries 10 transmembrane α-helical domains, thus works as a proton pump on the plasma membrane (Toyoshima et al., 2000). It gets energy from ATP hydrolysis for active transport of protons out to cells, and

generates the cation gradient. This activity of Pma1 is necessary for cells to uptake nutrients, including carbohydrates and amino acids, from the environment through the H+ cotransporter pathway. Because of this important role, Pma1 is essential for yeast cells to survive (Goffeau and Slayman, 1981; Rao et al., 1992).

In this study, I obtained a mutant form of yeast Pma1, namely Pma1-2308, which was not transported to the cell surface. Pma1-2308 formed and was accumulated in the ERAC structures on the ER. This mutant form of Pma1 was co-localized with mammalian CFTR on the same ERACs in yeast cells. Meanwhile, unlike CTFR and other ERAC-forming proteins, when highly expressed, Pma1-2308 considerably induced the UPR pathway, suggesting that it causes robust ER damage.

4-phenyl butyric acid (4-PBA) is a chemical chaperone that can prevent protein aggregation. More importantly, 4-PBA was reported to suppress the UPR in both yeast and mammal (Kubota et al., 2006a; Le et al., 2016). I thus checked the effect of this chemical chaperone on ERAC formation and the UPR caused by Pma1-2308. My results showed that 4-PBA disperses the ERAC and spreads Pma1-2308 across the ER when applied into yeast culture. Intriguingly, 4-PBA further increased the level of the UPR and cell death caused by the Pma1-2308 expression. This observation indicates a beneficial aspect of the ERAC formation. I speculate that the ERAC is a sequestration site for misfolded proteins, which may be more toxic for cells when diffusively distributed over the ER.

II. MATERIALS AND METHODS

2.1. Plasmid construction

Plasmid pTH761-CEN-mCherry_v4 contains a yeast codon-optimized version of the mCherry cDNA (Chu et al., 2014). The human CFTR cDNA was a gift from Prof. Kenji Kohno (Nara Inst. Sci. Tech.). Using these cDNAs as templates, I obtained the mCherry-coding and the CFTR-coding DNA fragments through high-fidelity PCR with Pyrobest DNA polymerase (Takara). The Pma1-coding DNA fragment was PCR-amplified from a yeast genome using conventional Takara ExTaq DNA polymerase.

The yeast centromeric plasmid pPM28 (*URA3* marker; Merksamer et al., 2008) was used for expression of eroGFP under control of the *TDH3* plasmid. After NheI/XbaI digestion, which resulted in excision of the eroGFP-coding sequence, pPM28 was ligated with the Pma1-coding and the mCherry-coding DNA fragments or the CFTR-coding and the mCherry-coding DNA fragments. The resulting plasmids, pYT-TDH3p-PMA1-mCherry and pYT-TDH3p-CFTR-mCherry, respectively, were used for expression of wild-type Pma1-mCherry and CFTR-mCherry in yeast cells. Due to PCR error, I also obtained the *PMA1-2308* mutant version of pYT-TDH3p-PMA1-mCherry, which is named pYT-TDH3p-PMA1-2308-mCherry. The *CUP1* promoter sequence was PCR-amplified from the yeast genome and was substituted on the *TDH3* promoter of pYT-TDH3p-PMA1-2308-mCherry for generation of pYT-CUP1p-PMA1-2308-mCherry, which was used for expression of Pma1-2308-mCherry under the control of the *CUP1* promoter in yeast cells. The 13-tandem-copy Myc epitope-coding sequence was PCR-amplified from the plasmid pFA6a-13Myc-kanMX6 (Bahler et al., 1998), and was substituted on the mCherry-coding sequence of pYT-CUP1p-PMA1-2308-mCherry for generation of pYT-CUP1p-PMA1-2308-Myc, which was used for expression of Pma1-2308-Myc under the control of the *CUP1* promoter in yeast cells. These plasmids were deposited in the Yeast Genetic Resource Center (YGRC), and the plasmid sequence information is available in the dropbox site (https://www.dropbox.com/sh/ocqptzlcfafq7t0/AACA61a-YeaTkJSigzmJbUhwa?dl=0) and on the YGRC website (http://yeast.nig.ac.jp/yeast/top.xhtml). For the empty vector control, pRS316 (Sikorski and Hieter, 1989) was employed.

The hemagglutinin (HA) epitope-tagged Ire1-gene centromeric (single-copy) plasmid pRS315-IRE1-HA, *IRE1*-gene centromeric (single-copy) plasmid pRS313-IRE1 and the empty vector pRS313 (*HIS3* marker) were described by Kimata et

al (2004) and Sikorski and Hieter (1989) (Kimata et al., 2004; Sikorski and Hieter, 1989).

2.2. Yeast strains

Unless otherwise noted, BY4742 (*MATα his3Δ1 leu2Δ0 lys2Δ0 ura3Δ0*) was used as a wild-type strain and transformed with the aforementioned plasmids. In the experiments using 4-PBA, KMY1516 (*MATα his3 leu2 lys2 ura3 trp1 ire1::TRP1 leu2::UPRE-GFP::LEU2 lys2::UPRE-lacZ::LYS2*; Kimata et al., 2004) carrying pRS313-IRE1 was employed as a wild-type strain and transformed with the aforementioned plasmids, because the viability of BY4742 was somewhat sensitive to 4-PBA (data not shown). For the *IRE1* gene-knockout experiments, KMY1516 cells transformed with pRS313-IRE1 and pRS313, respectively, were used as the *IRE1+* and the *ire1Δ* strains. For cellular expression of Ire1-HA, I employed KMY1015 (*MATα his3 leu2 lys2 ura3 trp1 ire1::TRP1*; Mori et al., 1996) transformed with pRS315-IRE1-HA.

Transformation of the BY4742 cells with PvuI-digested pYT-CUP1p-PMA1-2308-mCherry together with NotI-digested pRS315 (*LEU2* marker) (Sikorski and Hieter, 1989) yielded the *LEU2*-marker version of pYT-CUP1p-PMA1-2308-mCherry via *in vivo* homologous recombination. The resulting transformants were again transformed with pPM28 in order to obtain cells producing both Pma1-2308-mCherry and eroGFP.

BY4742-derived *HRD1/DOA10*-double knockout strain (*hrd1::kanMX4 doa10::SpHIS5MX*) has been described previously (Mai et al., 2018), and here was transformed with pYT-TDH3p-CFTR-mCherry. Alternatively, this *HRD1/DOA10*-double knockout strain was modified to carry both the *LEU2*-marker version of pYT-CUP1p-PMA1-2308-mCherry and the mCherry-to-GFP replaced version of pTDH3p-CFTR-mCherry, which were also generated through *in vivo* homologous recombination.

Yeast transformation was performed using the standard lithium-acetate-based protocol (Kaiser et al., 1994).

Table 1. List of strains used in this study

Name	Description	Source
BY4742	*MATα his3Δ1 leu2Δ0 lys2Δ0 ura3Δ0*	(Winston et al., 1995)

KMY1516	*MATα his3 leu2 lys2 ura3 trp1 ire1::TRP1 leu2::UPRE-GFP::LEU2 lys2::UPRE-lacZ::LYS2*	(Kimata et al., 2004)
KMY1015	*MATα his3 leu2 lys2 ura3 trp1 ire1::TRP1*	(Mori et al., 1996)
TKY007	*MATα his3Δ1 leu2Δ0 lys2Δ0 ura3Δ0 hrd1::kanMX4 doa10:: SpHIS5MX*	(Mai et al., 2018)

2.3. Yeast culture

Unless otherwise noted, yeast cells were aerobically and exponentially shaken in synthetic dextrose (SD) medium containing 2% glucose, 0.66% Difco Yeast Nitrogen Base (w/o amino acid) and appropriate auxotrophic requirements at 30 °C. Alternatively, cells were cultured at 23 °C to obtain brighter CFTR-mCherry or CFTR-GFP signals. SD medium plates containing 2% agar were incubated at 30 °C after inoculation of yeast cells. For chemical treatment of cells, tunicamycin (Sigma-Aldrich; 2 mg/mL in dimethyl sulfoxide for stock solution), CuO_4 (0.5 M in water for stock solution), and 4-PBA (Sigma-Aldrich; 0.5 M in water for stock solution) were added into cultures, which were further shaken at 30°C.

2.4. Protein and RNA analyzes

After harvested by centrifugation at 1,600 Xg for 1 min, approximately 5.0 OD_{600} cells for lysates or 40 OD_{600} cells for IP samples, were disrupted by agitation with glass beads (425-600 μm) in 100 μl of the lysis buffer containing 50mM Tris-Cl (pH7.9), 5 mM ethylenediaminetetraacetic acid and 1% Triton X-100 and protease inhibitors (2mM phenylmethylsulfonyl fluoride, 100 μg/ml leupeptin, 100 μg/ml aprotinin, 20 μg/ml pepstatin A and Calbiochem Protease Inhibitor cocktail Set III (X100 dilution)). Then cell lysates or IP samples were clarified by centrifugation at 8,000 Xg for 10 min. Cell lysates were fractionated by standard SDS-DTT polyacrylamide gel electrophoresis (PAGE), and transferred onto the polyvinylidene difluoride-based Western-bolotting membrane (Hybond-P; GE Healthcare). The semi-dry electrophoretic transfer and subsequent treatment of the blot membranes were performed as indicated by manufacturer's instruction. For Western blotting, I used mouse monoclonal antibodies 12CA5 (anti-HA epitope; Roche) and 9E10 (anti-c-Myc epitope anti-HA antibody (anti-c-Myc; Roche). In the experiment shown in Fig. 17C, cell lysates were centrifuged at 15,000 × *g* for 30 min to obtain pellet fractions. In order to denature proteins, I

added 10% trichloroacetic acid (TCA) and 100 mM dithiothreitol (DTT) into the SDS poly-acrylamide gel electrophoresis (SDS-PADE) loading buffer in the experiments shown in Figs. 10, 11A and 17C.

IP samples were mixed with 800 µl IP buffer (60 mM Tris-HCL pH 7.9; 6 mM EDTA;180 mM NaCl; 1% Triton X-100) with 6% skim milk and 10 µl of Myc-antibody. After being incubated at 4°C overnight, samples were centrifuged at 8000 xg for 10 min. Supernatants were incubated with 15 µl of protein A–conjugated Sepharose beads (Protein A Sepharose 4 FF; Amersham Biosciences, Uppsala, Sweden) for 1 hour at 4°C. Beads then were collected by 3000 xg centrifugation and washed 5 times by wash buffer (50 mM Tris-HCL pH 7.9; 5 mM EDTA;150 mM NaCl; 1% Triton X-100) and used as immunoprecipitate samples.

The hot-phenol method was employed for extraction of total RNA from yeast cells (Kimata et al., 2003). In order to monitor the *HAC1*-mRNA splicing, we subjected the total RNA sample to the reverse transcriptase (RT)-PCR analysis using the 17-mer polyA primer for the RT reaction and the *HAC1* specific primers for the PCR reaction (Mai et al., 2018; Promlek et al., 2011).

Table 2. List of oligonucleotides used in this study

Name	Sequence	Binding to
Oligo dT	TTTTTTTTTTTTTTTT	mRNA
Forward *HAC1*	TACAGGGATTTCCAGAGCACG	HAC1 sequence
Reverse *HAC1*	TGAAGTGATGAAGAAATCATTCAATTC	HAC1 sequence

The resulting RT-PCR were electrophoretically run on 2% agarose gel, which were then stained with ethidium bromide and observed under the fluorescence imager GelDoc XR+ system (BioRad). The ethidium bromide-fluorescence images of the resulting gels was used for image analysis which was followed by calculation of "the *HAC1* mRNA-splicing efficiency" using the formula [100 × (band intensity of $HAC1^{i}$)/{(band intensity of $HAC1^{i}$) + (band intensity of $HAC1^{u}$)}], where $HAC1^{i}$ and $HAC1^{u}$, respectively, are the spliced and unspliced forms of the *HAC1* mRNA.

2.5. Microscopic observation

In order to stain cells with 5-(and-6-)-carboxy-2',7'-dichlorofluorescein diacetate (carboxy-DCFDA), cells were suspended in sodium citrate buffer (pH 5.0) containing 2% glucose and 10 mM carboxyl-DCFDA for 30 min.

I observed yeast cells under the Keyence BZ-9000E microscope and the objective lens CFI Plan Apo λ100xH (Nikon). GFP and carboxy-DCFDA fluorescence was observed using a preset filter set (excitation wavelength, 470/30; dichroic mirror wavelength, 495; emission, 535/25). The mCherry fluorescence was observed using another preset filter set (excitation wavelength, 560/20; dichroic mirror wavelength, 595; emission, 630/30). The exposure time was 0.5 or 1.0 sec for wild-type Pma1-mCherry or Pma1-2308-mCherry fluorescence, 1.0 sec for eroGFP fluorescence, 8 sec for CFTR-mCherry fluorescence and 0.8 sec for carboxy-DCFDA fluorescence.

In order to quantitatively express ER dispersion of Pma1-2308-mCherry, I counted cells showing nuclear-ER unbroken ring-like fluorescent image of Pma1-2308-mCherry. More than 50 fluorescence-emitting cells were checked per sample, and its portion against total fluorescence-emitting cells are expressed as the mean of three independent cultures.

2.6. Flow cytometry

The flow cytometer Accuri C6 Plus (BD Biosciences) were operated under the following conditions: flow rate, slow; threshold, FCS-H > 80,000; count cell number, 20,000. In order to count propidium iodide (PI)-stainable cells, cultures were mixed with PI (10 μg/mL (final concentration)), further incubated for 30 min and subjected to flow cytometry.

2.7. Statistical analysis

Numerical data were obtained through multiple (basically three) determinations using independent clones, and were evaluated by the unpaired (homoscedastic) two-tailed *t*-test.

III. RESULTS

3.1. A mutant version of Pma1, Pma1-2308, forms the ERACs.

At the beginning of this study, I constructed a yeast expression plasmid (pYT-TDH3p-PMA1-mCherry) to produce a C-terminally mCherry-tagged version of Pma1 (Pma1-mCherry) under the control of the strong and constitutive *TDH3* promoter. As shown in Figs 4 and 5, mCherry fluorescence was observed in the cell periphery and the vacuoles, which were stained by the vacuole-staining dye carboxy-DCFDA, of yeast cells harboring this plasmid. This florescence pattern was consistent with that reported by Eastwood and Meneghini (2015) and suggests that Pma1-mCherry on the plasma membrane was partly subjected to endocytosis and transported to the vacuoles. (Eastwood and Meneghini, 2015)

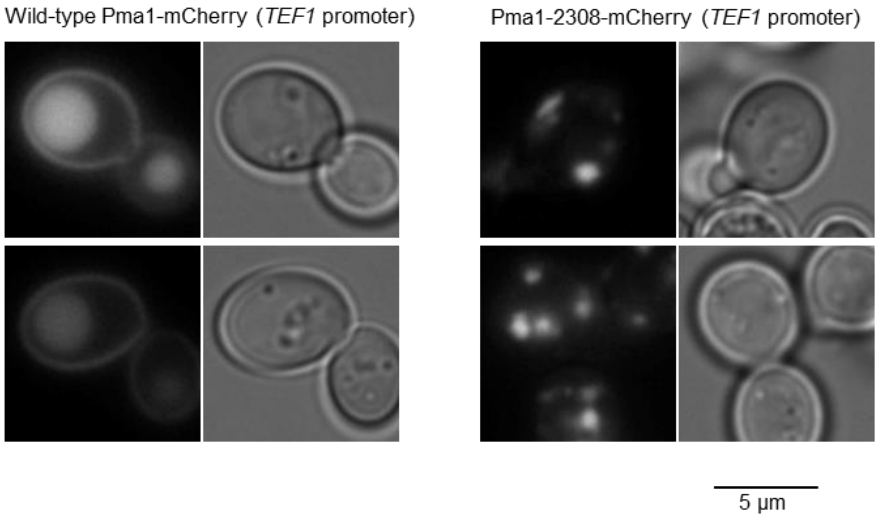

Figure 4. Wild-type Pma1-mCherry and Pma1-2308-mCherry show different localization in yeast cells. Wild-type cells producing wild-type Pma1-mCherry or Pma1-2308-mCherry under *TDH3*-promoter control were observed under fluorescence microscopy

Since I yielded the *PMA1* gene through PCR in which the DNA replication fidelity was low (see the Materials and Methods section) to construct pYT-TDH3p-PMA1-mCherry, I also obtained a *PMA1* gene-mutant version of this plasmid. Since the mutation frequency was fairly high, I obtained this mutant through observing only a few clones. Based on the mutation-site detection described in the next paragraph, I named this mutant as *PMA1-2308*. Expression of Pma1-2308 is likely to harm cells since yeast cells transformed with the *PMA1-2308* mutant variant of pYT-TDH3p-PMA1-mCherry (pYT-TDH3p-PMA1-2308-mCherry)

proliferated very slowly (Fig. 6). Intriguingly, unlike wild-type Pma1-mCherry, Pma1-2308-mCherry exhibited a punctate distribution pattern, which did not merge with the vacuole marker, in yeast cells (Figs 4 and 5). Although I obtained this mutant unexpectedly and by chance, its phenotypes described in this paragraph led me to start my research that is presented throughout this thesis.

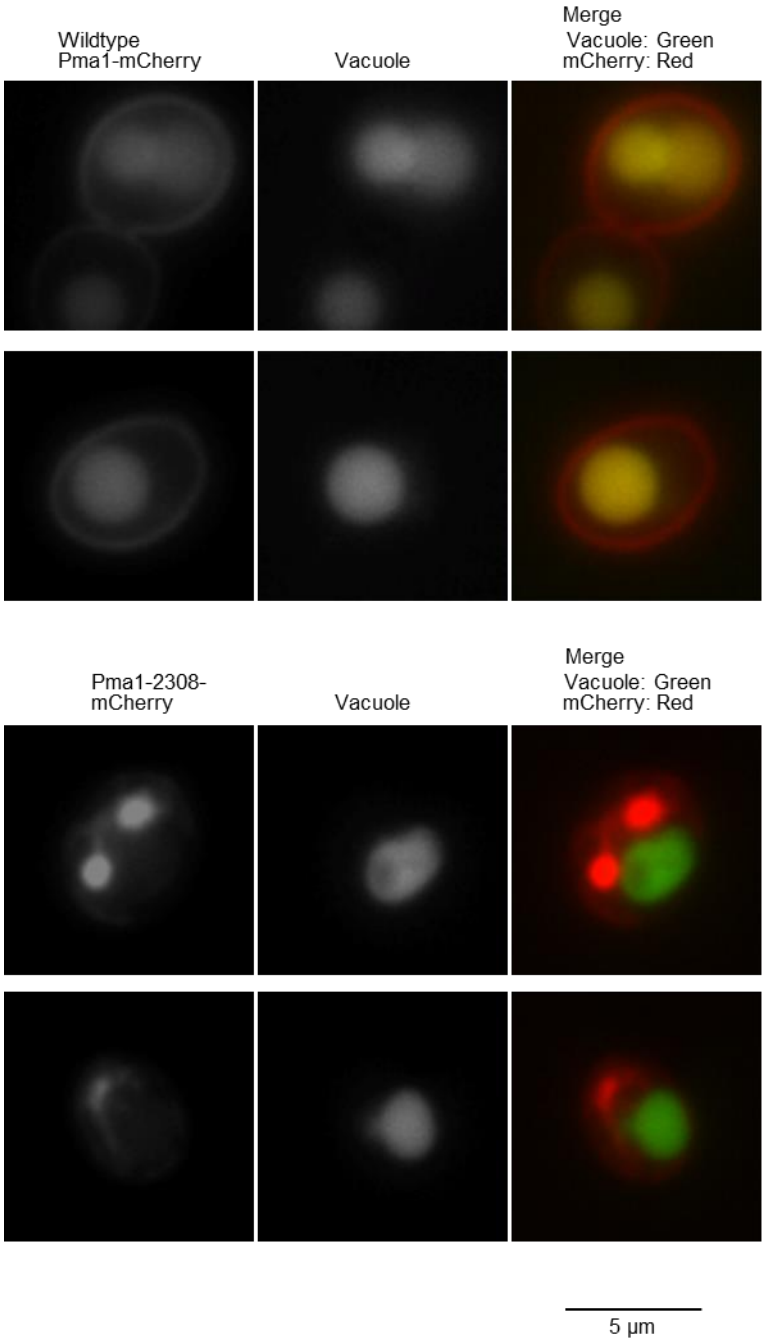

Figure 5. Wild-type Pma1-mCherry, but not Pma1-2308mCherry, is partly located to the vacuoles. Wild-type cells producing wild-type Pma1-mCherry (under *TDH3*-promoter control) or those producing Pma1-2308-mCherry (under *CUP1*-promoter control; cultured with 500 μM $CuSO_4$ for 4 hr) were stained with the vacuole marker dye carboxyl-DCFDA and observed under fluorescence microscopy.

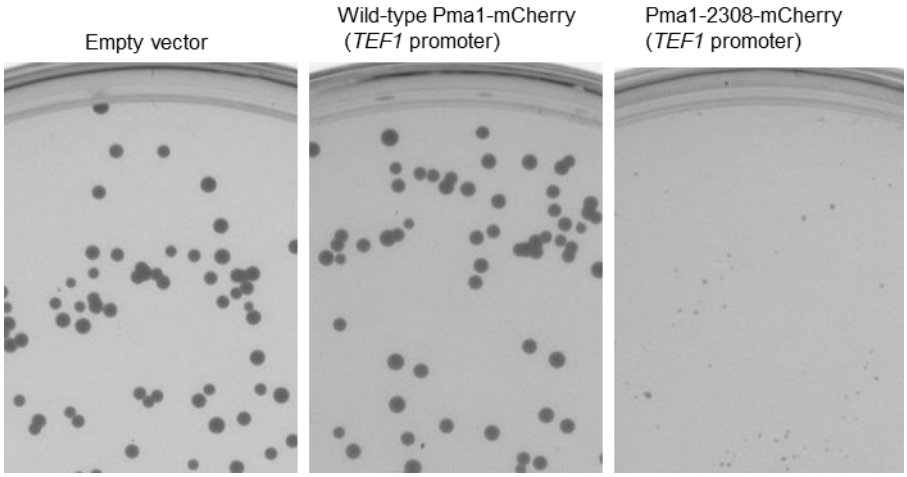

Figure 6. Cellular expression of Pma1-2308-mCherry causes growth retardation. After being cultured in liquid SD medium, wild-type cells carrying the wild-type Pma1-mCherry expression plasmid (*TDH3* promoter), the Pma1-2308-mCherry expression plasmid (*TDH3* promoter) or the empty vector were plated onto SD agar plates, which were pictured after 2.5-days' incubation.

The *PMA1-2308* mutant carried one silent (non-amino acid-replacing) nucleotide replacement (Thymine1548-to-Cytosine) and four non-silent (amino acid-replacing) nucleotide replacements which are indicated in Fig. 7A (the nucleotides are numbered from the initiation codon of the *PMA1* gene). In order to determine which is responsible for the punctum-forming phenotype of the *PMA1-2308* mutation, I introduced each of the non-silent nucleotide replacements into the wild-type Pma1-mCherry gene. As shown in Fig. 7A, Pma1-mCherry exhibited a punctate distribution when carrying the Thymine 2308-to-Cytosine single mutation, which corresponds to Serine 770-to-Proline replacement of the Pma1 protein. It should be also noted that the Serine 770-to-Proline replacement was also responsible for the growth-retardation phenotype of the *PMA1-2308* mutation (Fig. 7B). In agreement to this point, as described later, another phenotype of *PMA1-2308*, namely induction of the UPR, is also likely to be caused by the Serine 700-to-Proline mutation.

In order to grow yeast cells carrying the *PMA1-2308* gene to an extent that sufficiently allowed the below-mentioned experiments, I constructed yeast cells in which Pma1-mCherry-2308 was expressed from an inducible promoter. As expected, yeast cells transformed with pYT-CUP1p-PMA1-2308-mCherry, from which expression of Pma-2308-mCherry was regulated under the control of the copper ion-inducible *CUP1* promoter, exhibited fluorescence when cultured in the presence of 500 μM $CuSO_4$ (Fig. 8). According to my flowcytometric analysis (Fig.

9), the expression level of Pma1-2308-mCherry reached a maximum level 4-hr after induction onset under my experimental condition.

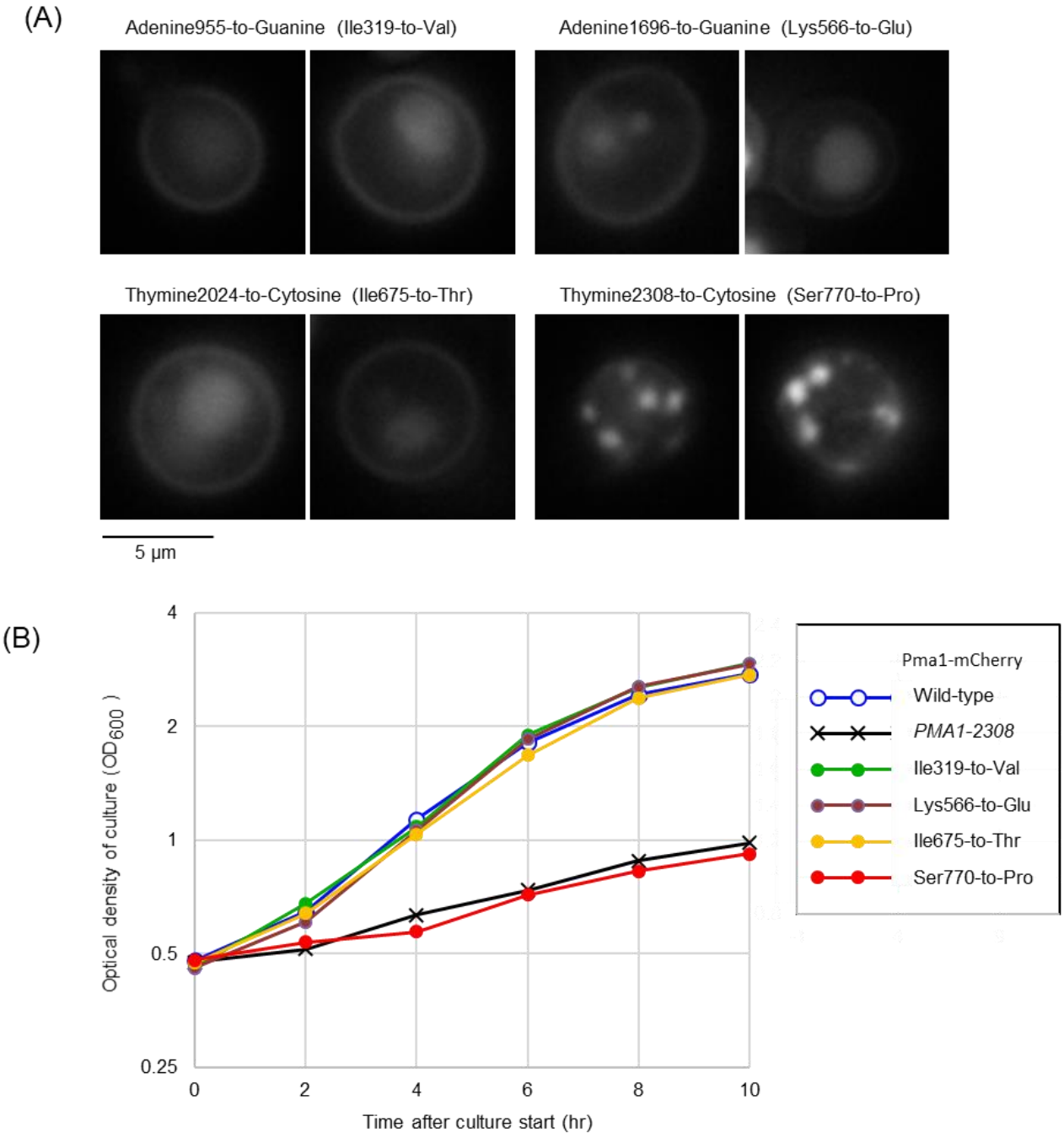

Figure 7. The Thymine2308-to-Cytosine (Serine770-to-Proline) replacement is responsible for the ERAC-forming and growth-retardation phenotypes of *PMA1-2308*. (A) Wild-type cells producing Pma1-mCherry carrying the indicated single point mutations (under *TDH3*-promoter control) were observed under fluorescence microscopy. (B) Wild-type cells producing wild-type Pma1-mCherry, Pma1-2308-mCherry or Pma1-mCherry carrying the indicated single point mutations (under *TDH3*-promoter control) were checked for growth in liquid medium.

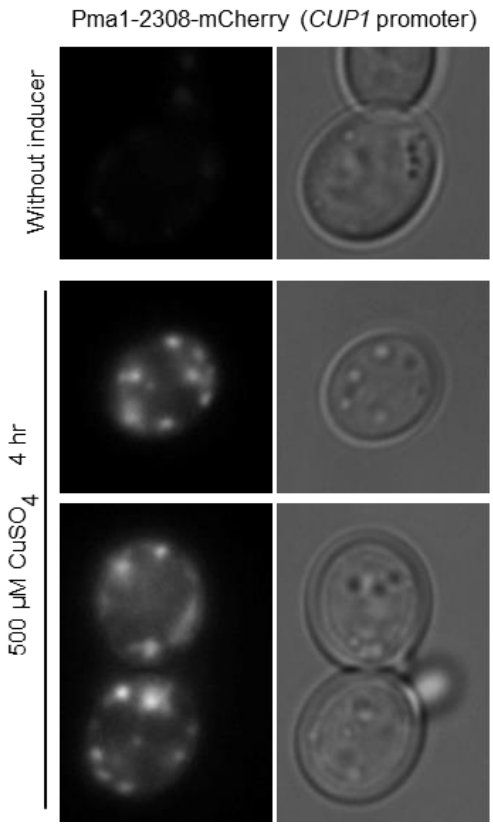

Figure 8. Cellular expression of Pma1-2308-mCherry under the *CUP1* promoter control. Wild-type cells that produce Pma1-2308-mCherry under *CUP1*-promoter control were cultured with or without 500 μM $CuSO_4$ for 4 hr and observed under fluorescence microscopy.

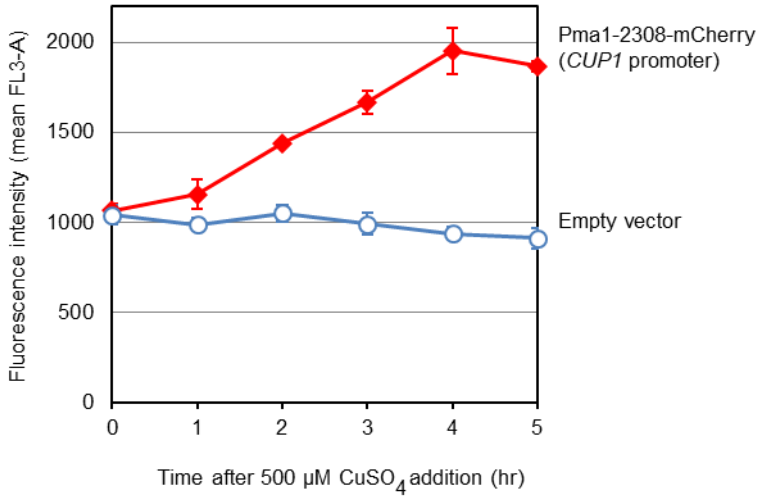

Figure 9. Expression profile of Pma1-2308-mCherry under the control of the *CUP1* promoter. Wild-type cells carrying the Pma1-2308-mCherry expression plasmid (*CUP1* promoter) or the empty vector were cultured with 500 μM $CuSO_4$ for the indicated durations and were analyzed by flowcytometry.

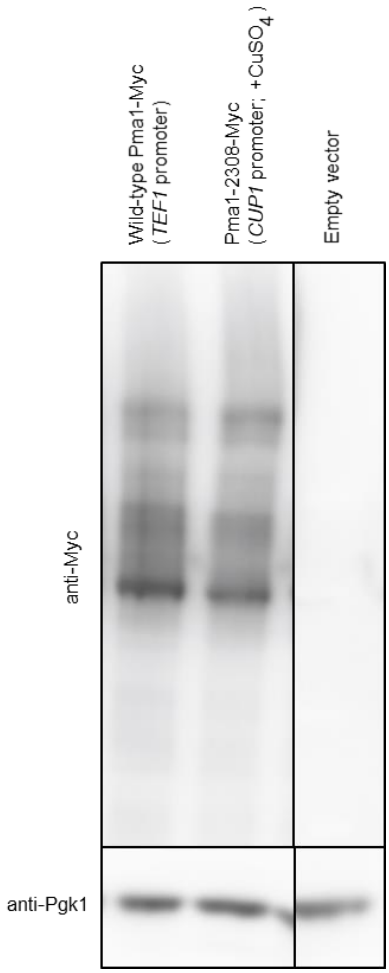

Figure 10. Wild-type Pma1-Myc and Pma1-2308-Myc exhibit similar band pattern on SDS/DTT-PAGE. Total cell lysates from wild-type cells producing wild-type Pma1-Myc (under *TDH3*-promoter control) and from those producing Pma1-2308-mCherry (under *CUP1*-promoter control; cultured with 500 μM $CuSO_4$ for 4 hr) were analyzed by anti-Myc Western blotting. Each lane contained sample from cells equivalent to OD_{600}=0.13. Four panels are from the same blot membrane. Anti-Pgk1 Western blot served as a loading control.

In the experiment shown in Fig. 10, the C-terminally Myc-epitope-tagged versions of wild-type Pma1 (wild-type Pma1-Myc) and Pma1-2308 (Pma1-2308-Myc) were expressed in wild-type cells, the lysates of which were analyzed by anti-Myc Western blotting. Although protein samples were denatured by SDS, DTT and TCA before electrophoresis (see the Materials and Methods section), Pma1-2308-Myc, as well as wild-type Pma1-Myc, appeared as slightly laddered and smeared bands for unknown reason(s) (Fig. 10). I next checked stability of wild-type Pma1-Myc and Pma1-2308-Myc using the cycloheximide-chase technique. According to my data shown in Fig. 11, Pma1-2308-Myc seemed to be fairly stable (more stable than wild-type Pma1-Myc) in yeast cells.

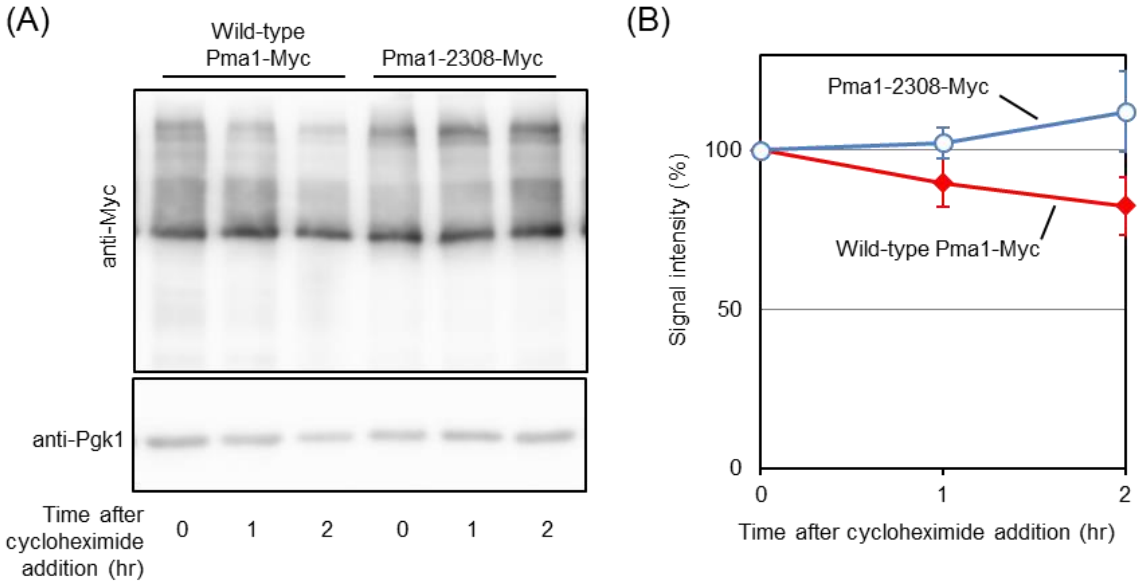

Figure 11. Cycloheximide chase assay for monitoring stability of wild-type Pma1-Myc and Pma1-2308-Myc. (A) Wild-type Pma1-Myc was produced under *TDH3*-promoter control in wild-type cells. Pma1-2308-mCherry was produced under *CUP1*-promoter control in wild-type cells (Cell were cultured with 500 μM $CuSO_4$ for 4 hr before this assay). Cycloheximide (250 μg/mL (final concentration)) was then added into the cultures, which were further cultured for the indicated durations and were analyzed through anti-Myc Western blotting of cell lysates. Each lane contained sample from cells equivalent to OD_{600}=0.13. Anti-Pgk1 Western blot served as a loading control. (B) Signal intensity of wild-type Pma1-Myc and Pma1-2308-Myc of the cycloheximide chase assay is measured and presented. The values of the t=0 samples are set at 100%.

In the experiment shown in Fig. 12, I observed yeast cells expressing both (or either) Pma1-2308-mCherry and eroGFP, which is an ER-localized variant of GFP (Merksamer et al., 2008). When expressed alone in yeast cells, eroGFP showed a typical double-ring ER distribution pattern. On the other hand, eroGFP was also distributed to punctate dots that were located on or adjacent to the double rings when it was expressed together with Pma1-2308-mCherry. It should be also noted that Pma1-2308-mCherry was located on the eroGFP puncta. I thus deduce that Pma1-2308-mCherry forms and is accumulated in the ERACs, as described in the Discussion section.

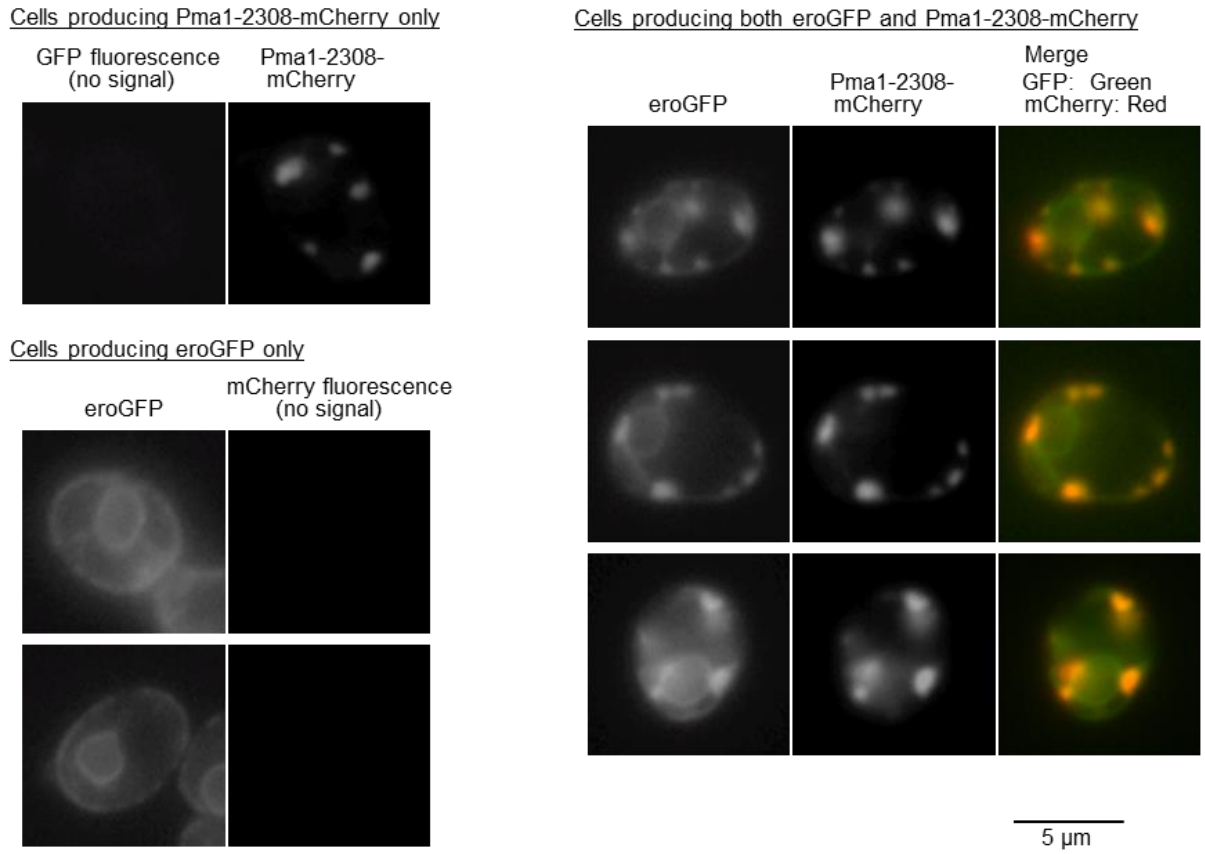

Figure 12. Pma-2308-mCherry exhibits a dot-like distribution on the ER. Wild-type cells that produce both (or either) Pma1-2308-mCherry (under *CUP1*-promoter control) and eroGFP (under *TDH3*-promoter control) were cultured with 500 μM $CuSO_4$ for 4 hr and observed under fluorescent microscopy.

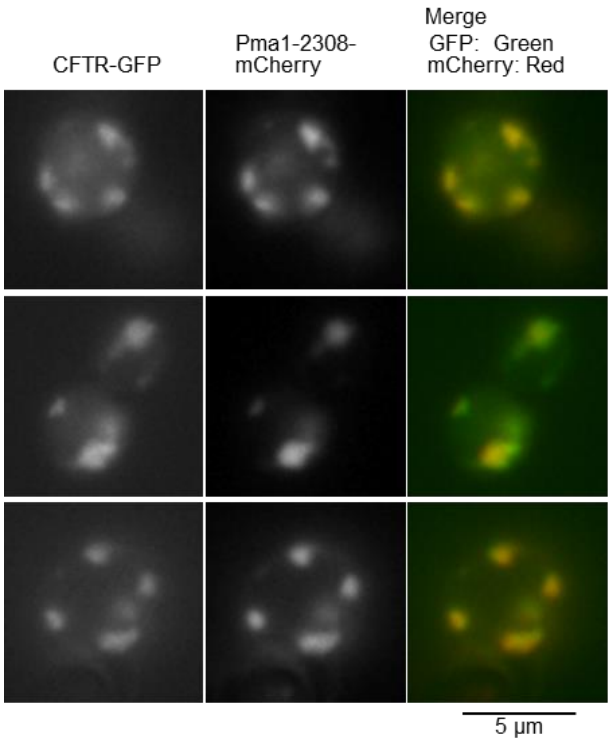

Figure 13. Pma1-2308 and CFTR co-localize in the same ERACs. *hrd1Δdoa10Δ* cells that produce both Pma1-2308-mCherry (under *CUP1*-promoter control) and CFTR-GFP (under *TDH3*-promoter control) were cultured with 500 μM $CuSO_4$ for 4 hr and observed under fluorescent microscopy.

As described in the Introduction section, heterogenously expressed CFTR is also located in the ERACs in yeast cells. In order to observe intracellular localization of C-terminally GFP-tagged CFTR (CFTR-GFP), I employed here the *hrd1Δ*/*doa10Δ* double deletion mutant strain because CFTR-GFP is quickly degraded through the ER-associated protein degradation in a manner dependent on the E3 enzymes Hrd1 and Doa10 (Gnann et al., 2004) and hardly emits observable fluorescence in wild-type yeast cells. As shown in Fig. 13, CFTR-GFP and Pma1-2308-mCherry were co-localized, indicating that these two different ERAC-forming proteins are accumulated in the same ERACs.

3.2. Pma1-2308 damages cells at least partly through inducing ER stress.

Next, I asked if cellular expression of Pma1-2308-mCherry induces ER stress that triggers the UPR, which is monitorable through the *HAC1* mRNA splicing. As described previously (Mai et al., 2018; Promlek et al., 2011), here I amplified the *HAC1* spices from total RNA samples using the reverse transcription (RT)-PCR technique. Fig. 14A shows that Pma1-2308-mCherry, but not wild-type Pma1-mCherry, triggered *HAC1*-mRNA splicing when it was expressed from the *TDH3* promoter. According to my data shown in Fig. 15, the Serine 770-to-Proline replacement was responsible for the ER-stressing phenotype of the *PMA1-2308* mutation. This data is consistent with the aforementioned observation that the growth-retardation phenotype of *PMA1-2308* is also due to the Serine 770-to-Proline replacement on this gene.

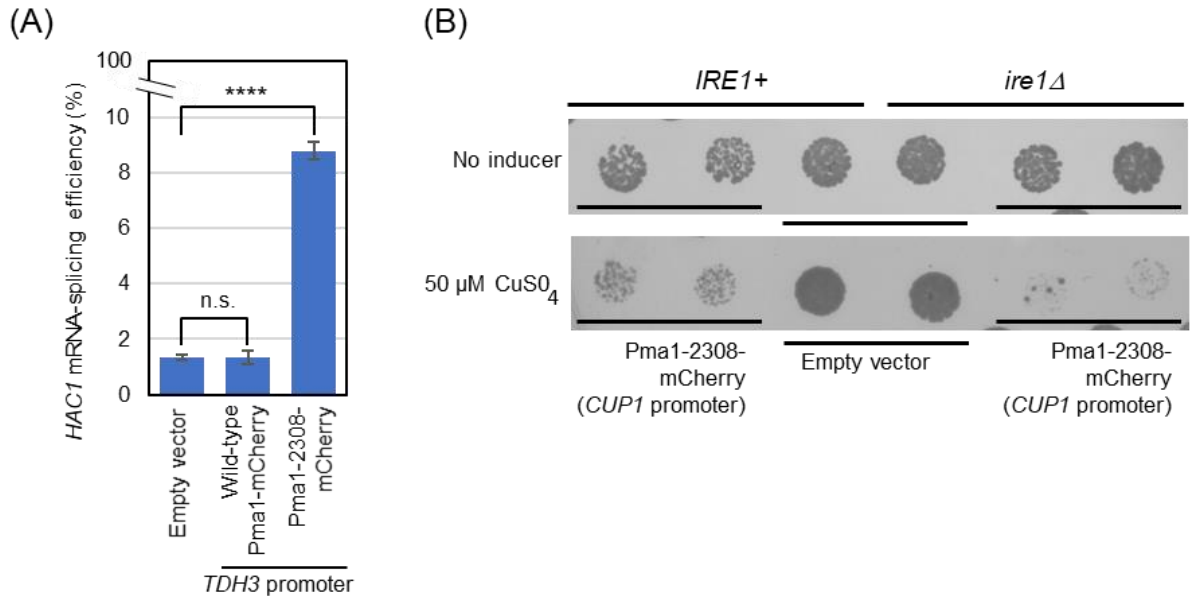

Figure 14. Pma1-2308 induces the UPR. (A) Wild-type cells producing either (or neither) wild-type Pma1-mCherry or Pma1-2308-mCherry under the *TDH3*-promoter control were checked for *HAC1* mRNA-splicing efficiency. ****: p<0.001, n.s.: not significant (p>0.05). (B) *IRE1+* and *ire1*Δ cells carrying the *CUP1* promoter-controlled Pma1-2308-mCherry expression plasmid or the empty vector were spotted on SD agar plates supplemented or not with 50 μM CuO_4, which were then incubated for 3 days. On each spot, cells equivalent to OD_{600}=0.00015 were inoculated.

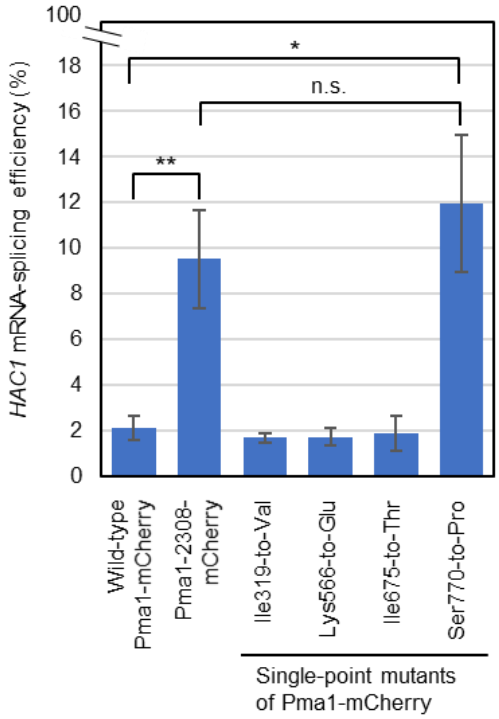

Figure 15. The Serine770-to-Proline replacement is responsible for the ER-stressing phenotypes of *PMA1-2308*. Wild-type cells producing wild-type Pma1-mCherry, Pma1-2308-mCherry or Pma1-mCherry carrying the indicated single point mutations (under *TDH3*-promoter control) were checked for *HAC1* mRNA-splicing efficiency. **: p<0.01, *: p<0.05, n.s.: not significant (p>0.05).

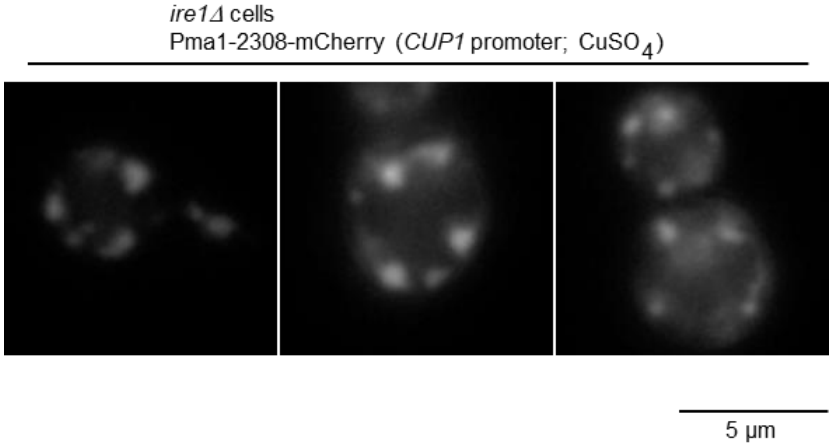

Figure 16. ERAC formation of Pma1-2308-mCherry in *ire1*Δ cells. *ire1*Δ cells carrying the Pma1-2308-mCherry expression plasmid (*CUP1* promoter) were cultured with 500 μM $CuSO_4$ for 4 hr and were observed under fluorescence microscopy.

UPR induction by the Pma1-2308-mCherry expressed from the *CUP1* promoter is described later in this thesis. In the experiment shown in Fig. 14B, cells were grown on agar media containing or not containing an inducible concentration of $CuSO_4$. Cells carrying the *CUP1* promoter-controlled Pma1-2308-mCherry-expression plasmid showed growth retardation, which was aggravated by the absence of the *IRE1* gene, on the inducer-containing plate. These observations indicate that, at least partly, Pma1-2308-mCherry harms yeast cells through induction of ER stress.

Fig. 16 exhibits the ERAC formation of Pma1-2308-mCherry in *ire1Δ* cells. In other words, while involved in the mitigation of cellular damage induced by the ERAC-forming protein Pma1-2308, the UPR is not required for the ERAC-formation of Pma1-2308 *per se*.

3.3. 4-PBA works as a chemical chaperone in yeast cells when applied at a proper concentration.

4-phenylbutyric acid (4-PBA) is known as a chemical chaperone that prevents protein aggregation (Kolb et al., 2015; Kubota et al., 2006b; Ranga Rao et al., 2018). Reportedly, 4-PBA suppresses the UPR in both yeast and mammalian cells (Kubota et al., 2006b; Le et al., 2016; Ozcan et al., 2006). I then asked how 4-PBA affects the ERAC formation and the UPR induction by Pma1-2308 when added into yeast cultures.

Before addressing this question, in the experiment shown in Fig. 17A, I checked if I can reproduce the UPR-suppressing effect of 4-PBA. Yeast cells were

cultured in the presence or absence of a canonical ER-stressing reagent tunicamycin, and were checked for the *HAC1*-mRNA splicing. In agreement with the aforementioned previous reports, the *HAC1*-mRNA splicing was completely suppressed when 5mM 4-PBA was added in to yeast cultures 15 min before the tunicamycin addition. In this experiment, cells were cultured with 4-PBA for 75 min, as done previously in my laboratory (Le et al., 2016; Mai et al., 2018). Because Ire1 is the key factor for the *HAC1*-mRNA splicing, I next checked if the cellular abundance of Ire1 is affected by 4-PBA at this concentration, In the experiment shown in Fig. 17B, I employed cells producing C-terminally HA-epitope-tagged Ire1 (Ire1-HA), the lysates of which were analyzed by anti-HA Western blotting. I then found that the cellular abundance of Ire1-HA was decreased by culturing cells with 5-mM 4-PBA. Therefore, it is possible that at least partly, 4-PBA suppresses the *HAC1*-mRNA splicing by decreasing the cellular level of Ire1. This may be an undesirable side effect of 4-PBA as a chemical chaperone to cope with ER-accumulated unfolded proteins.

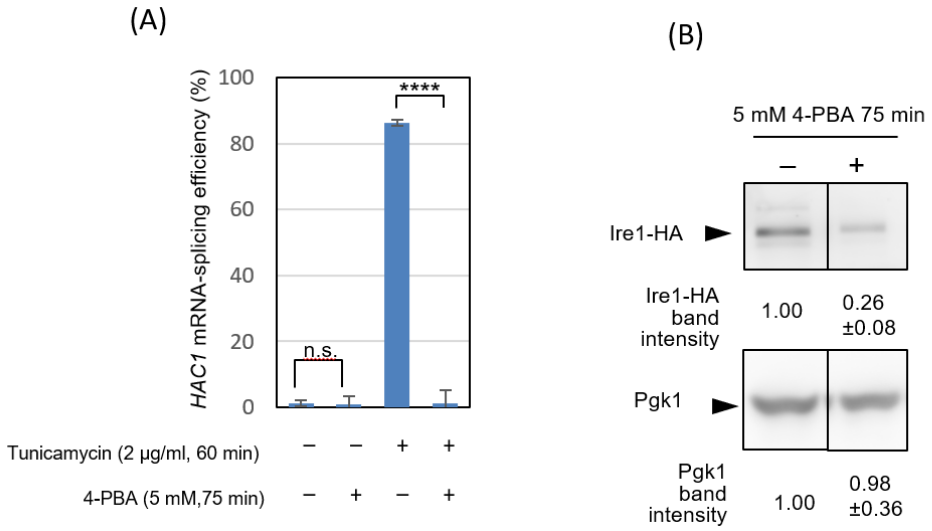

Figure 17. 5 mM 4-PBA suppresses the *HAC1*-mRNA splicing of yeast cells partly and possibly through decreasing the cellular abundance of Ire1. (A) Wild-type cells were treated with 2 μg/mL tunicamycin for 1 hr. 5 mM 4-PBA was added 15 min before tunicamycin addition. Cells were then checked for *HAC1*-mRNA splicing. ****: $p<0.001$, n.s.: not significant ($p>0.05$). (B) Cells producing Ire1-HA were treated with 5 mM 4-PBA for 75 minutes or left untreated, and the total lysates from the cells (equivalent to OD_{600}=0.13) were analyzed by anti-HA Western blotting. Anti-Pgk1 Western blot served as a loading control.

In order to avoid this side effect of 4-PBA, I added 4-PBA at different concentrations. As shown in Fig. 18A, 4-PBA suppressed the *HAC*-mRNA splicing almost completely even when it was added into yeast cultures at a concentration

of 1 mM. Importantly, under this condition, 4-PBA decreased the cellular abundance of Ire1-HA only slightly (Fig. 18B). Hereafter, I thus used this concentration of 4-PBA for exertion of its effect as a chemical chaperone.

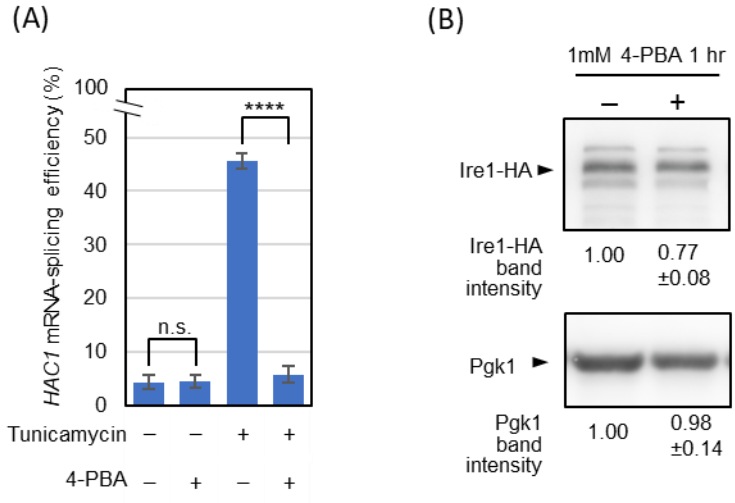

Figure 18. 1 mM 4-PBA suppresses tunicamycin-induced UPR without causing a drastic decrement of the cellular abundance of Ire1. (A) Wild-type cells were treated with 2 μg/mL tunicamycin and/or 1 mM 4-PBA for 1 hr, and were checked for *HAC1*-mRNA splicing. ****: $p<0.001$, n.s.: not significant ($p>0.05$). (B) Cells producing Ire1-HA were treated with 1 mM 4-PBA for 1 hr or left untreated, and the total lysates from cells (equivalent to $OD_{600}=0.13$) were analyzed by anti-HA Western blotting. Anti-Pgk1 Western blot served as a loading control.

3.4. 4-PBA inhibits ERAC formation by Pma1-2308.

I therefore set the working concentration of 4-PBA at 1 mM, and checked if 4-PBA affects the cellular localization of the ERAC-forming proteins. As shown in Figs 19A and B, treatment of cells with 1 mM 4-PBA caused dispersed distribution of Pma1-1192-mCherry and C-terminally mCherry-tagged CFTR (CFTR-mCherry). Since cellular distribution of Pma1-1192-mCherry and CFTR-mCherry in 4-PBA-treated cells seemed to be the typical double-ring-like ER pattern, we deduce that, at least partly, they are retained in the ER without being transported to the cell surface.

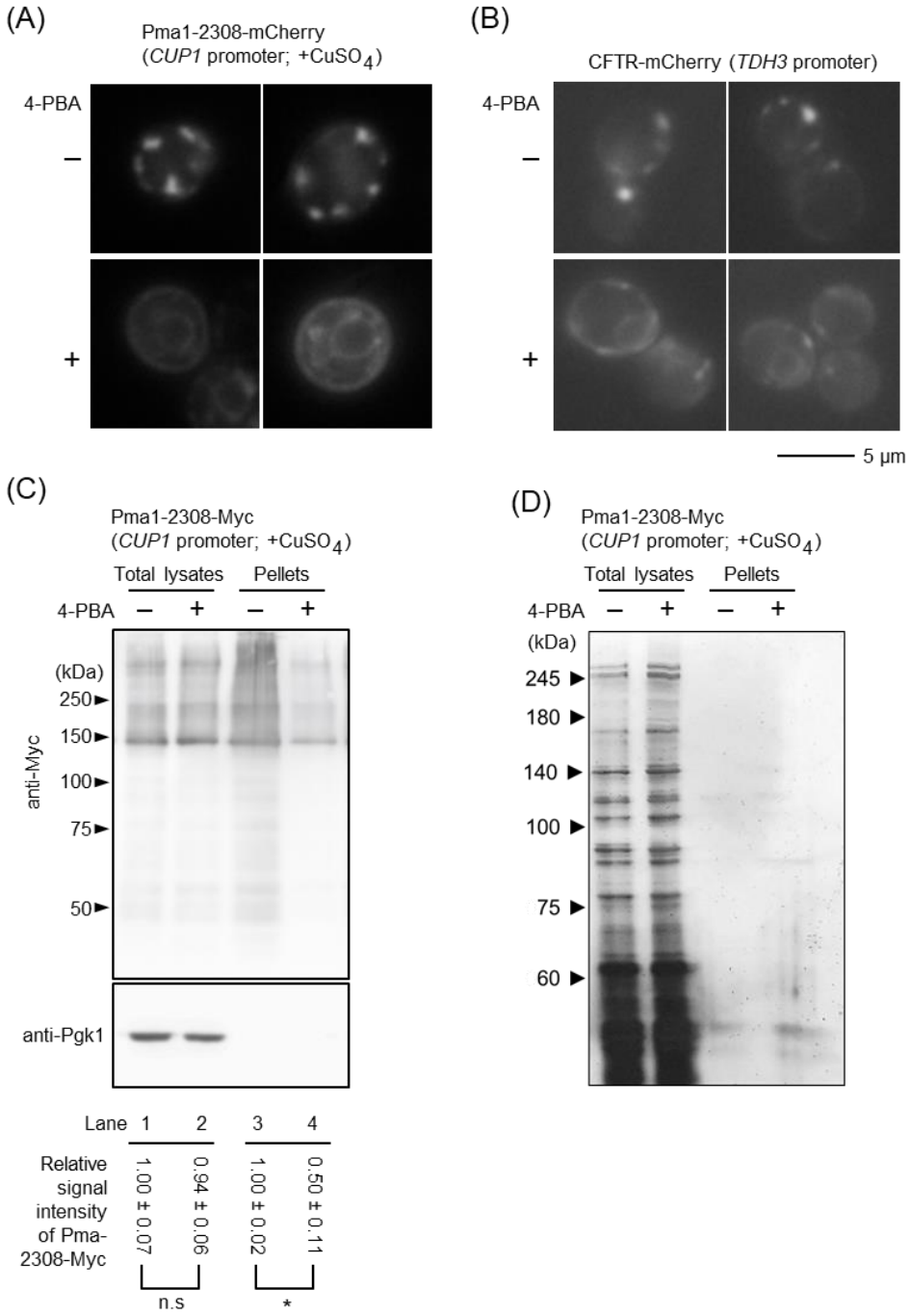

Figure 19. 4-PBA compromises the ERAC formation. (A) Cells that produce Pma1-2308-mCherry under *CUP1*-promoter control were cultured with 500 μM $CuSO_4$ and 1 mM 4-PBA (or with 500 μM $CuSO_4$ only) for 4 hr and observed under fluorescence microscopy. (B) *hrd1Δdoa10Δ* cells producing CFTR-mCherry under *TDH3*-promoter control were cultured with or without 500 μM 4-PBA for 3 hr and observed under fluorescence microscopy. (C) Cells that produce Pma1-2308-Myc under *CUP1*-promoter control were cultured with 500 μM $CuSO_4$ and 1 mM 4-PBA (or with 500 μM $CuSO_4$ only) for 4 hr and lysed in the presence of 1% Triton-X100. The total cell lysates were then separated by high-speed centrifugation and analyzed by anti-Myc Western blotting. Each lane contained sample from cells equivalent to OD_{600}=0.13 for "total lysates" and from cells equivalent to OD_{600}=2.5 for "pellets." Anti-Pgk1 Western blot served as a loading control. (D). The samples in (C) were subjected to SDS-PAGE, and the gel was stained by sliver staining.*: $p<0.05$, n.s.: not significant ($p>0.05$).

In the experiment shown in Fig. 19C, lysates of cells producing Pma1-2308-Myc were subjected to anti-Myc Western blotting, indicating that treatment of cells with 4-PBA did not significantly change the cellular abundance of Pma1-2308-Myc (compare Lane 2 to Lane 1). I also subjected the total cell lysates to high-speed centrifugation and noticed that cellular treatment with 4-PBA decreased the abundance of Pma1-2308-Myc in the pellet fractions (compare Lane 4 to Lane 3). Probably because Pgk1, a commonly used loading control, is a soluble protein, Pgk1 bands were not observed on the pellet-sample lanes in Fig. 19C. As a loading control for Fig. 19C, we thus silver stained the gel instead of performing the Western-blot analysis (Fig. 19D). As expected, the two pellet samples, as well as the two total-lysate samples, showed similar band patterns in Fig. 19D.

Next, I asked if 4-PBA can disperse already-ERAC-forming Pma1-2308-mCherry proteins. In the experiment shown in Fig. 20, yeast cells producing Pma1-2308-mCherry from the *CUP1* promoter through 4-hr culture with 500 μM $CuSO_4$ were washed with normal medium and further cultured in the absence of an inducible concentration of $CuSO_4$ (chase culturing). I then found that Pma1-2308-mCherry was dispersed, though not completely, when chase culturing was performed in the presence of 1 mM 4-PBA. In order to express this observation quantitatively, I counted cells showing dispersed distribution of Pma1-2308-mCherry, which was represented by its nuclear-ER unbroken ring-like image (Fig. 20).

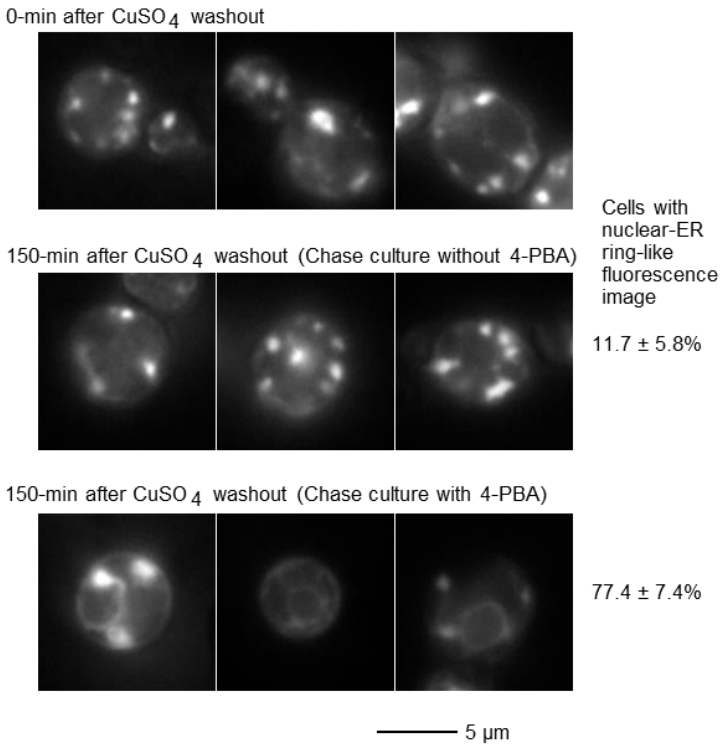

Figure 20. 4-PBA disperses Pma1-2308-mCherry already forming the ERACs. After being cultured in the presence of 500 μM $CuSO_4$, cells producing Pma1-2308-mCherry under *CUP1*-promoter control were washed four times with SD medium ($CuSO_4$ washout) and further incubated in the presence or absence of 1 mM 4-PBA for 150 min (chase culture).

Next, I asked if a chemical chaperone other than 4-PBA can inhibit ERAC formation. In the experiment shown in Fig. 21, trehalose was added into yeast cultures at different concentrations, which showed no inhibitory effect for the ERAC formation of Pma1-2308.

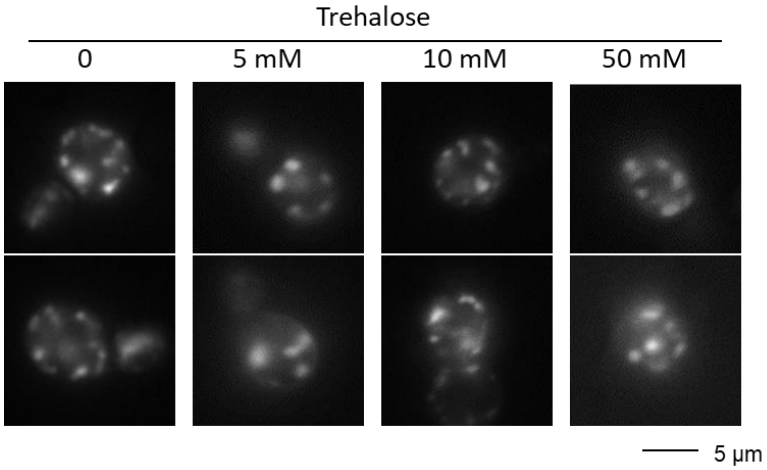

Figure 21. Trehalose does not compromise the ERAC formation of Pma1-2308. Cells producing Pma1-2308-mCherry under *CUP1*-promoter control were cultured with $CuSO_4$ (500 μM) plus trehalose (5, 10 or 50 mM) or with 500 μM $CuSO_4$ only for 4 hr and were observed under a fluorescence microscope.

3.5. 4-PBA aggravates ER stress and cell damage caused by Pma1-2308.

In the next part of this study, I asked if ER stress is alleviated or aggravated when the ERAC formation of Pma1-2308-mCherry is compromised by cellular treatment with 4-PBA. In order to monitor the effect of 4-PBA on the cellular UPR level, I employed the experimental condition represented in Fig. 22A, in which yeast cells were treated with 1 mM 4-PBA for no longer than 1 hr (4-PBA was added 3-hr after addition of 500 μM $CuSO_4$ into culture). Fig. 22B shows that, under this condition, Pma1-2308-mCherry was partially dispersed. Notably, 4-PBA further increased the UPR level that was induced by Pma1-2308-mCherry, at least under the experimental procedure employed here (Fig. 22C). I therefore deduce that the dispersion of Pma1-2308-mCherry by 4-PBA aggravates ER stress. This observation is in contrast with the case of stressing yeast cells with the canonical ER stressor tunicamycin, in which 4-PBA compromised the UPR (Fig. 18A). In the experiments shown in Fig. 22, I avoided treatment of yeast cells with 4-PBA for a longer duration, which decreased the cellular Ire1 abundance (data not shown), possibly leading to a reduction of the *HAC1*-mRNA level and to an underestimation of the cellular ER-stress level. PI is known to stain dead yeast cells (Kwolek-Mirek and Zadrag-Tecza, 2014). In the experiment shown in Fig.

22D, I measured the portion of PI-stainable cells in cultures and found that the cellular expression of Pma1-2308-mCherry caused a reduction of cell viability, which was aggravated by 4-PBA. These phenomena are unlikely to be results toxicity of $CuSO_4$, since $CuSO_4$ alone induced neither the UPR level nor cell death in the case of negative-control cells not carrying the Pma1-2308-mCherry gene (Fig. 23).

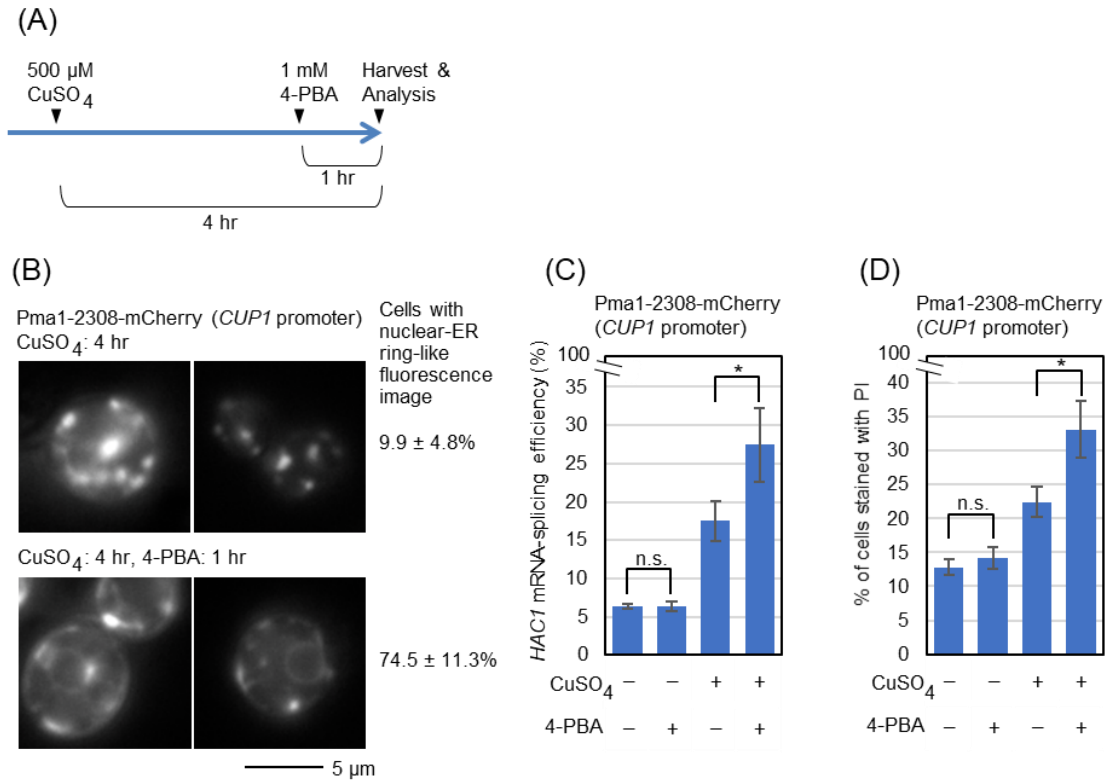

Figure 22. 4-PBA enhances the UPR induced by Pma1-2308-mCherry. (A) Procedure for treatment of cells with 4-PBA 3 hr-after the induction onset of Pma1-2308-mCherry expression. (B) Cells that produce Pma1-2308-mCherry under *CUP1*-promoter control were treated as shown in panel A, and were observed under fluorescence microscopy. (C) and (D) Cells that produce Pma1-2308-mCherry under *CUP1*-promoter control were treated as shown in panel A (or cultured with either or none of the chemicals), and were checked for the *HAC1*-mRNA splicing (C) or the portion of PI-stainable cells in the cultures (D). *: $p<0.05$, n.s.: not significant ($p>0.05$).

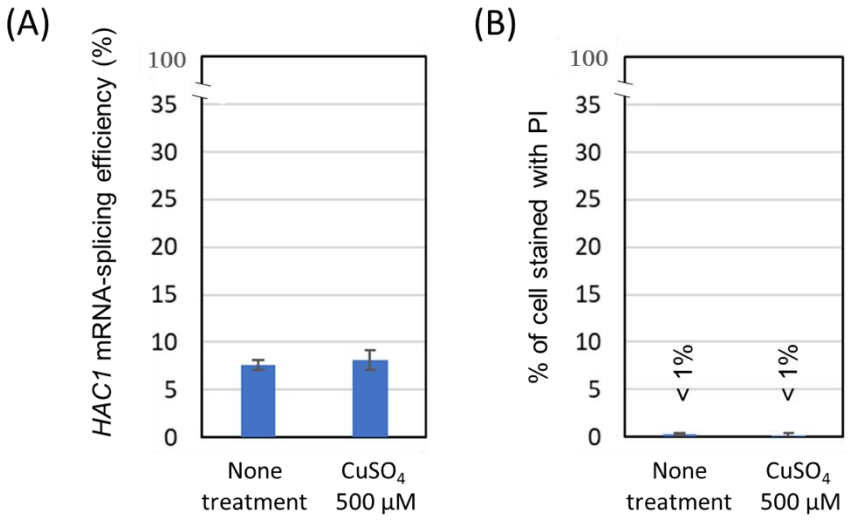

Figure 23. $CuSO_4$ *per se* does not induce *HAC1* splicing or cell death. Wild-type cells not carrying Pma1-2308-mCherry expression plasmid (*CUP1* promoter) were treated with 500 μM CuSO4 for 4 hours, then were checked for the *HAC1*-mRNA splicing (A) or the portion of PI-stainable cells in the cultures (B).

3.6. Further investigations to elucidate the properties of the yeast ERACs

In order to understand the properties of the ERACs more deeply, I have performed two other experiments in this final part of my study. The first is a trial to find a protein(s) that physically interacts to Pma1-2308 but not to wild-type Pma1. In the experiment shown in Fig. 24, lysates of cells producing either wild-type Pma1-Myc or Pma1-2308-Myc were subjected to anti-Myc immunoprecipitation, which are followed by SDS-PAGE and the silver staining. The protein association profiles of these two samples were no largely different (compare lane 5 and 6). I thus failed to detect a specific interaction of Pma1-2308 to other proteins.

In the second experiment, I asked if wild-type cells form ERAC-like structures without excessive and artificial expression of mutant proteins. I treated wild-type cells producing eroGFP, the ER marker, with various stress-inducing reagents and observed them under a fluorescence microscope. While cellular treatment with ER stressors, DTT or tunicamycin, did not change the ER morphology (data not shown), sodium azide caused ERAC-like puncta formation in yeast cells (Fig. 25).

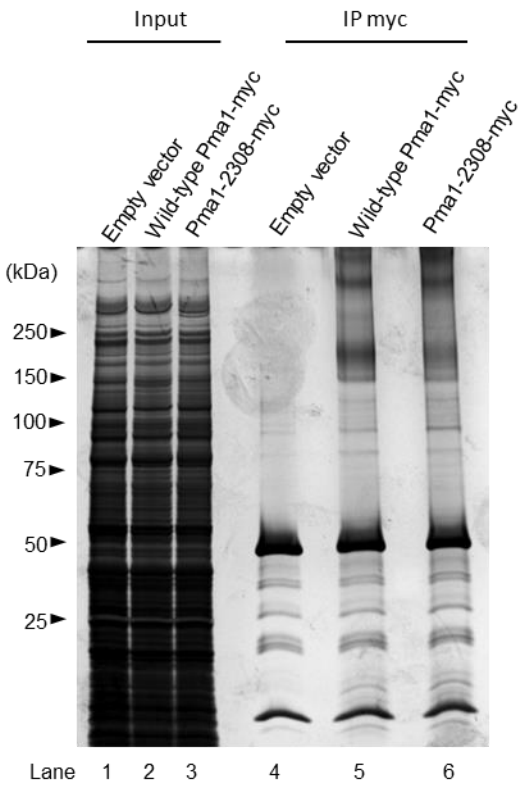

Figure 24. Protein-association profile of wild-type and mutant Pma1. Cells producing Pma1-2308-Myc or wild-type Pma1-Myc under *CUP1*-promoter were cultured with 500 μM $CuSO_4$ for 4 hr, and were collected for preparation of their lysates, which were subjected to anti-Myc immunoprecipitation (IP). Lysates and IP samples were separated by SDS-PAGE and were stained by sliver staining.

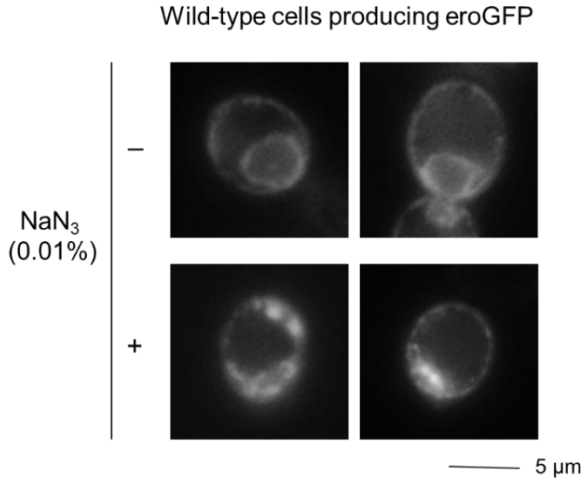

Figure 25. Formation of ERAC-like structures in wild-type yeast cell. Wild-type cells producing eroGFP were treated by NaN_3 with the final concentration of 0.01% for 2 hr and were observed under a fluorescence microscope.

IV. DISCUSSION

To my knowledge, the ERAC formation in yeast cells was initially reported by Huyer et al. (2004). The ERACs are defined as ER subcompartments in which misfolded multimembrane-spanning proteins are localized. The ER is a flat-shaped membranous sac, which, according to the electron microscopic images reported by Huyer et al. (2004) and Fu and Sztul (2009), is partly folded and stacked to form multiple layers on the site where the ERACs are formed. This observation is consistent with my fluorescence microscopy images of yeast cells producing both eroGFP, which is thought to be diffusively located in the ER, and Pma1-2308-mCherry (Fig. 12). In yeast cells producing both fluorescent proteins, eroGFP fluorescence displayed faint double rings and bright puncta adjacent to the rings, and Pma1-2308-mCherry was located on the eroGFP puncta. It should be also noted that Pma1-2308-mCherry and heterogenously expressed CFTR were co-localized (Fig. 13). To my knowledge, this is the first report showing that two different ERAC-forming proteins are accumulated in the same ERACs.

As aforementioned, some previous studies on the yeast ERACs employed CFTR or mutant Ste6 as model ERAC-forming proteins. Probably because these proteins are unstable and are degraded quickly through the ERAD or autophagy when expressed in yeast cells, they did not induce the yeast UPR (Fua and Sztula, 2009; Huyer et al., 2004; Kakoi et al., 2013). Unlike those ERAC-forming proteins, Pma1-2308-mCherry was stable (Fig. 11) and clearly induced the UPR in yeast cells (Figs 14A and 22C), indicating that Pma1-2308-mCherry damages the ER. On the other hand, my data showing in Fig. 16 demonstrates that the UPR signaling pathway is dispensable for the ERAC formation of Pma1-2308-mCherry. In addition, cytotoxicity of Pma1-2308-mCherry was enhanced by the *IRE1*-gene deletion (Fig. 14B). It is widely accepted that, in general, the *IRE1*-gene deletion aggravates cellular damage caused by ER-stressing stimuli (Kubota et al., 2006a; Le et al., 2016; Miyagawa et al., 2014; Umebayashi et al., 1997).

I speculate the difference in the UPR inducibility between CFTR and Pma1-2308 may be simply due to their cellular abundance, which probably reflects the difference in their stability. In agreement with the insights concerning protein stability that is described in the foregoing paragraph, I noticed that CFTR-mCherry exhibited far darker fluorescent signal than Pma1-2308-mCherry even when they were expressed from the same gene-expression promoters in yeast cells (data not shown). In other words, ERAC-forming proteins other than Pma1-2308-mCherry may exert cytotoxicity as well as Pma1-2308-mCherry, if it is abundantly

accumulated in yeast cells. This possibility should be experimentally addressed in future, because at present, there is only weak counterevidence against an idea that the cytotoxicity argued here may be a specific story only about my Pma1 mutant but not about other ERAC-forming proteins.

As described in Kubota et al. (2006), 4-PBA is likely to function as a chemical chaperone that prevents aggregation of denatured proteins. Moreover, 4-PBA suppresses the UPR in mammalian and yeast cells, and is thought to be a promising chemical that can be used for therapeutic purposes for various diseases caused by ER accumulation of misfolded proteins (Kolb et al., 2015; Kubota et al., 2006a). However, I reported previously and presented here that at least in yeast cells, 4-PBA compromises the UPR not via restoration of the protein folding status in the ER but via reduction of the cellular Ire1 abundance (Fig. 17, Mai et al., 2018). Meanwhile, here I employed a lower concentration of 4-PBA than that was used in previous publications by me and others (Kubota et al., 2006a; Mai et al., 2018), and found that 4-PBA suppresses the tunicamycin-induced UPR without reduction of the cellular Ire1 abundance (Figs 18). Intriguingly, 4-PBA extinguished the ERACs and caused a dispersed distribution of ERAC-forming proteins across the ER (Figs 19 and 20). Therefore, I conclude that 4-PBA can actually work as a molecular chaperone in yeast cells when applied at appropriate concentrations. However, it should be also noted that 4-PBA is an amphipathic small molecule, which is likely to interact with various biological molecules and to exert unexpected side effects, leading to degradation of Ire1, when it is applied at higher concentrations.

In the experiment shown in Fig. 19C, I separated cell lysates through high-speed centrifugation, and found that the amount of Pma1-2308-Myc in the pellet fraction was decreased by cellular treatment with 4-PBA. I deduce that accumulation of Pma1-2308-Myc in the pellet fraction, which was compromised by 4-PBA, represents its aggregation. Taken together, my observations support the notion that the ERACs are formed through aggregation of ERAC-forming proteins. In agreement with this idea, the fluorescence-recovery-after-photobleaching analysis performed by Fu et al. (2009) showed that in yeast cells, the CFTR becomes less mobile when accumulated into the ERACs.

Intriguingly, the UPR induced by Pma1-2308-mCherry was aggravated by 4-PBA (Fig. 22C). Moreover, viability of cells expressing Pma1-2308-mCherry was decreased by 4-PBA (Fig. 22D). Since, as described above, 4-PBA disperse the ERACs, I assume that these findings represent a beneficial aspect of the ERAC formation. It should be also noted the cellular abundance of Pma1-2308 was

almost unaffected by 4-PBA (Fig. 19C). In other words, 4-PBA increased cytotoxicity of Pma1-2308 not through increasing its cellular abundance. On the other hand, I cannot exclude a possibility that 4-PBA enhances the Pma1-2308-induced ER stress and its resulting cytotoxicity by another reason. In other words, 4-PBA may be potentially ER-stressing, and may cause a cellular damage which additively or synergistically induces ER stress and harms cells together with cellular expression of Pma1-2308.

Nevertheless, it should also be noted, at least in the case of other ER-stressing stimuli, including cellular treatment with tunicamycin, the UPR was attenuated by 4-PBA (Fig. 18; Kubota et al., 2006; Le et al., 2016). Moreover, according to Kubota et al. (2006), 4-PBA supports cellular growth of *ire1Δ* cells in the presence of tunicamycin. These observations demonstrate an effect of 4-PBA to mitigate ER stress, and thus argue against the aforementioned idea that 4-PBA *per se* is potentially ER stressing.

According to the transmission electron microscopic analysis performed by Huyer et al. (2004), the ER is heavily stacked to form the REACs. Huyer et al. (2004) also noted that, although not frequently, local stacking of the ER is observable even in wild-type yeast cells not genetically modified to produce ERAC-forming aberrant proteins. Here I checked ER morphology in wild-type cells fluorescence microscopically using eroGFP as the ER marker (Fig. 25), and found that sodium azide, an inhibitor of ATPase, induces formation of ERAC-like puncta (Fig. 25). We speculate that depletion of ATP leads to misfolding of endogenous transmembrane proteins, which form the ERACs. In other words, the ERACs can be formed even without artificial expression of ERAC-forming aberrant proteins when cells encounter certain severe stressing stimuli. Although probably less seriously than sodium azide, various stressing stimuli, such as high temperature, aberrant osmotic pressure, toxic amino acid analogues, and oxidative stress, are likely to disturb cellular homeostasis, possibly leading to ATP depletion. A research question that should be addressed in future is if the ERACs are formed under these stressing conditions.

Another well-known chemical chaperone, trehalose, did not disperse ERACs (Fig. 21). This may be because trehalose and 4-PBA act in different ways. 4-PBA carries a hydrophobic moiety, which binds to exposed hydrophobic domains of unfolded proteins, and a hydrophilic moiety, which increases solubility of the bound proteins (Kolb et al., 2015). Trehalose is a disaccharide which can re-arrange water molecules around proteins and protect proteins from denaturation under extreme conditions, such as high temperature or dehydration (Lee et al.,

2018). Chemical compounds showing a mode of action similar to 4-PBA, such as lysophosphatidic acids, may have a 4-PBA-like activity to disperse the ERACs, which should be checked in future.

It should be noted that extracellularly supplemented trehalose is reported to protect yeast cells from other stressing stimuli, such as desiccation (Tapia et al., 2015). Moreover, Agt1 is likely to act as a plasma membrane-located trehalose transporter (Magalhães et al., 2018). While, based on these insights, I assume that trehalose was incorporated from medium to yeast cells in my experiment shown in Fig. 21, it is also possible that the medium-to-cell transport of trehalose was not efficient enough to allow trehalose to exert a biological effect(s).

Kamhi-Nesher et al. (2001) and Kondratyev et al. (2007) proposed that, in mammalian cells, model aberrant proteins are located in punctate ER subcompartments, which are named as the ER-derived quality control compartments (ERQCs) (Kamhi-Nesher et al., 2001; Kondratyev et al., 2007). It is uncertain if the yeast ERACs and the mammalian ERQCs are the identical or similar structures and play the same functions.

Taken together, in this study, I disclose some physiological properties of yeast ERACs by using a novel ERAC-forming model protein Pma1-2308. In contrast to the other previously known ERAC-forming proteins, Pma1-2308 was not degraded quickly, which allowed me to uncover a new aspect of the ERACs. I propose that the ERACs are formed through aggregation of aberrant multimembrane-spanning proteins, and work as sequestration sites of multiple client proteins, which are harmful for cells when diffusively distributed across the ER. One possible toxicity mechanism of dispersed unfolded proteins is that they may capture other normal proteins, which is then dysfunctioned. It is also possible that dispersed unfolded proteins may interact to nascent peptides and inhibit their proper folding. According to Kakoi et al. (2013), multiple cellular proteins, namely COPII-forming factors and cytosolic DnaJ-family proteins, are likely to contribute to the ERAC formation of CFTR. In agreement with my argument presented here, this insight suggests that yeast cells actively form the ERACs when aberrant multimembrane-spanning proteins are accumulated.

In order to understand the properties of the ERACs more deeply, I searched for proteins that interact to Pma1-2308, but failed (Fig. 24). Because CFTR and Pma1-2308 are located in the same ERACs (Fig. 13), I assume these two proteins form the ERACs through the same mechanism. In other words, COPII-forming factors and cytosolic DnaJ-family proteins may also be involved in the ERAC formation by Pma1-2308. By improving my technique to observe intracellular

protein-protein interaction, it may become possible to exhibit a physical interaction of Pma1-2308 to cytosolic DnaJ-family proteins, as well as that of CFTR (Kakoi et al., 2013), in yeast cells.

It should be noted that a common feature of the ERAC-forming proteins, namely CFTR, a Ste6 mutant, and Pma1-2308, is that they are all multi-membrane-spanning proteins. The ERAC-forming proteins may be highly self-oligomerized through intermolecular hydrophobic association of their transmembrane domains, resulting in the ERAC formation. On the other hand, by considering an involvement of cytosolic DnaJ-family proteins in the ERAC formation, it is also possible that some properties of its cytosolic segments designate a multi-membrane-spanning protein to be an ERAC-forming protein. In agreement with these idea, Ser770 is located on the cytosolic end of a transmembrane domain of Pma1.

While, as described so far, I assume that the essential nature of the ERACs formed by Pma1-2308 is not different from that of the ERACs formed by other ERAC forming proteins, namely CFTR and a Ste6 mutant, this assumption should be confirmed more doubtlessly in future. For instance, the morphological structure of the ERACs formed by Pma1-2308 should be checked by using the transmission electron microscopic technique. In addition, it is also an intriguing question if the COPII mutations impair the ERAC formation by Pma1-2308 as well as that by CFTR (Kakoi et al., 2013).

It is commonly accepted that improper or insufficient folding of proteins is problematic for cells, not only because unfolded or misfolded proteins cannot exert proper functions, but also because they are intrinsically hazardous. Unfolded proteins often form large aggregates, which can be a hallmark of a situation in which cells abundantly contain unfolded proteins. For instance, protein aggregates are observed in various human neurodegenerative diseases including Alzheimer's disease and Huntington's disease. In a study on the polyglutamine-based protein aggregation, which is a Huntington's-disease model, in yeast cells, toxicity of model aberrant proteins seemed to be positively link to their tendency to be aggregated (Gruber et al., 2018). Therefore, in a canonical understanding, protein aggregation is bad for cells. However, it is also possible that largely aggregated proteins are rather less toxic, since they are sequestered from other cellular components (Arrasate et al., 2004). My study presents an intriguing example in which an intracellular structure being associated with protein aggregation decreases the toxicity of an aberrant protein.

ACKNOWLEDGEMENT

Firstly, I would like to thank my supervisor – Associate Professor Yukio Kimata, who patiently taught me how to conduct a study and to work effectively as a researcher.

I would like to thank my advisors, Professor Kazuhiro Shiozaki, and Professor Hiroshi Takagi for their valuable time and helpful advices.

I would like to express my gratitude Takagi's lab members, especially Doctor Yuki Ishiwata-Kimata, for their kindly supports, not only in my work but also in my private life.

I truly appreciate the financial support from the Division of Biological Science at NAIST and from Japan Student Services Organization (JASSO), which make my doctoral study possible.

Finally, yet importantly, I want to say thanks to my family and friends for their encouragement and understanding.

Mai Chi Thanh

REFERENCES

Araki, K., and Nagata, K. (2011). Protein folding and quality control in the ER. Cold Spring Harb Perspect Biol *3*.

Arrasate M., Mitra S., Schweitzer E.S., Segal M.R., and Finkbeiner S. (2004). Inclusion body formation reduces levels of mutant huntingtin and the risk of neuronal death. Nature *431*, 805-810.

Bobadilla, J.L., Macek, M., Fine, J.P., and Farrell, P.M. (2002). Cystic fibrosis: a worldwide analysis of CFTR mutations--correlation with incidence data and application to screening. Hum Mutat *19*, 575–606.

Bustamante, H.A., González, A.E., Cerda-Troncoso, C., Shaughnessy, R., Otth, C., Soza, A., and Burgos, P.V. (2018). Interplay between the autophagy-lysosomal pathway and the ubiquitin-proteasome system: A target for therapeutic development in Alzheimer's disease. Front Cell Neurosci *12*.

Chu, D., Kazana, E., Bellanger, N., Singh, T., Tuite, M.F., and von der Haar, T. (2014). Translation elongation can control translation initiation on eukaryotic mRNAs. EMBO J *33*, 21–34.

Ciechanover, A. (2005). Proteolysis: from the lysosome to ubiquitin and the proteasome. Nat Rev Mol Cell Biol *6*, 79–87.

Cox, J.S., and Walter, P. (1996). A novel mechanism for regulating activity of a transcription factor that controls the unfolded protein response. Cell *87*, 391–404.

Credle, J.J., Finer-Moore, J.S., Papa, F.R., Stroud, R.M., and Walter, P. (2005). On the mechanism of sensing unfolded protein in the endoplasmic reticulum. Proc. Natl. Acad. Sci. U.S.A. *102*, 18773–18784.

Eastwood, M.D., and Meneghini, M.D. (2015). Developmental coordination of gamete differentiation with programmed cell death in sporulating yeast. Eukaryot Cell *14*, 858–867.

Escusa-Toret, S., Vonk, W.I.M., and Frydman, J. (2013). Spatial sequestration of misfolded proteins by a dynamic chaperone pathway enhances cellular fitness to stress. Nat Cell Biol *15*, 1231–1243.

Fua, L., and Sztula, E. (2009). ER-associated complexes (ERACs) containing aggregated cystic fibrosis transmembrane conductance regulator (CFTR) are degraded by autophagy. Eur J Cell Biol *88*, 215–226.

Gardner, B.M., and Walter, P. (2011). Unfolded proteins are Ire1-activating ligands that directly induce the unfolded protein response. Science *333*, 1891–1894.

Gnann, A., Riordan, J.R., and Wolf, D.H. (2004). Cystic fibrosis transmembrane conductance regulator degradation depends on the lectins Htm1p/EDEM and the Cdc48 protein complex in yeast. Mol Biol Cell *15*, 4125–4135.

Goffeau, A., and Slayman, C.W. (1981). The proton-translocating ATPase of the fungal plasma membrane. Biochimica et Biophysica Acta (BBA) - Reviews on Bioenergetics *639*, 197–223.

Gruber A., Hornburg D., Antonin M., Krahmer N., Collado J., Schaffer M., Zubaite G., Lüchtenborg C., Sachsenheimer T., Brügger B., Mann M., Baumeister W., Hartl F.U., Hipp M.S., and Fernández-Busnadiego R. (2018). Molecular and structural architecture of polyQ aggregates in yeast. Proc Natl Acad Sci U A. *115*, E3446-E3453.

Huyer, G., Longsworth, G.L., Mason, D.L., Mallampalli, M.P., McCaffery, J.M., Wright, R.L., and Michaelis, S. (2004). A striking quality control subcompartment in Saccharomyces cerevisiae: the endoplasmic reticulum-associated compartment. Mol Biol Cell *15*, 908–921.

Kaiser, C., Michaelis, S., and Aaron, M. (1994). Methods in yeast genetics : a Cold Spring Harbor Laboratory course manual.

Kakoi, S., Yorimitsu, T., and Sato, K. (2013). COPII machinery cooperates with ER-localized Hsp40 to sequester misfolded membrane proteins into ER-associated compartments. Mol Biol Cell *24*, 633–642.

Kamhi-Nesher, S., Shenkman, M., Tolchinsky, S., Fromm, S.V., Ehrlich, R., and Lederkremer, G.Z. (2001). A novel quality control compartment derived from the endoplasmic reticulum. Mol Biol Cell *12*, 1711–1723.

Karagöz, G.E., Acosta-Alvear, D., Nguyen, H.T., Lee, C.P., Chu, F., and Walter, P. (2017). An unfolded protein-induced conformational switch activates mammalian IRE1. Elife *6*.

Kimata, Y., Kimata, Y.I., Shimizu, Y., Abe, H., Farcasanu, I.C., Takeuchi, M., Rose, M.D., and Kohno, K. (2003). Genetic evidence for a role of BiP/Kar2 that regulates Ire1 in response to accumulation of unfolded proteins. Mol Biol Cell *14*, 2559–2569.

Kimata, Y., Oikawa, D., Shimizu, Y., Ishiwata-Kimata, Y., and Kohno, K. (2004). A role for BiP as an adjustor for the endoplasmic reticulum stress-sensing protein Ire1. J Cell Biol *167*, 445–456.

Kimata, Y., Ishiwata-Kimata, Y., Ito, T., Hirata, A., Suzuki, T., Oikawa, D., Takeuchi, M., and Kohno, K. (2007). Two regulatory steps of ER-stress sensor Ire1 involving its cluster formation and interaction with unfolded proteins. J. Cell Biol. *179*, 75–86.

Klionsky, D.J., Cregg, J.M., Dunn, W.A., Emr, S.D., Sakai, Y., Sandoval, I.V., Sibirny, A., Subramani, S., Thumm, M., Veenhuis, M., et al. (2003). A unified nomenclature for yeast autophagy-related genes. Dev Cell *5*, 539–545.

Kolb, P.S., Ayaub, E.A., Zhou, W., Yum, V., Dickhout, J.G., and Ask, K. (2015). The therapeutic effects of 4-phenylbutyric acid in maintaining proteostasis. Int J Biochem Cell Biol *61*, 45–52.

Kondratyev, M., Avezov, E., Shenkman, M., Groisman, B., and Lederkremer, G.Z. (2007). PERK-dependent compartmentalization of ERAD and unfolded protein response machineries during ER stress. Exp Cell Res *313*, 3395–3407.

Kubota, K., Niinuma, Y., Kaneko, M., Okuma, Y., Sugai, M., Omura, T., Uesugi, M., Uehara, T., Hosoi, T., and Nomura, Y. (2006a). Suppressive effects of 4-phenylbutyrate on the aggregation of Pael receptors and endoplasmic reticulum stress. Journal of Neurochemistry *97*, 1259–1268.

Kubota, K., Niinuma, Y., Kaneko, M., Okuma, Y., Sugai, M., Omura, T., Uesugi, M., Uehara, T., Hosoi, T., and Nomura, Y. (2006b). Suppressive effects of 4-phenylbutyrate on the aggregation of Pael receptors and endoplasmic reticulum stress. J. Neurochem. *97*, 1259–1268.

Kwolek-Mirek, M., and Zadrag-Tecza, R. (2014). Comparison of methods used for assessing the viability and vitality of yeast cells. FEMS Yeast Res *14*, 1068–1079.

Le, Q.G., Ishiwata-Kimata, Y., Kohno, K., and Kimata, Y. (2016). Cadmium impairs protein folding in the endoplasmic reticulum and induces the unfolded protein response. FEMS Yeast Res. *16*.

Lee, H.-J., Yoon, Y.-S., and Lee, S.-J. (2018). Mechanism of neuroprotection by trehalose: controversy surrounding autophagy induction. Cell Death Dis *9*, 712.

Lee, K.P.K., Dey, M., Neculai, D., Cao, C., Dever, T.E., and Sicheri, F. (2008). Structure of the dual enzyme Ire1 reveals the basis for catalysis and regulation in nonconventional RNA splicing. Cell *132*, 89–100.

Lousa, C. de M., and Denecke, J. (2016). Lysosomal and vacuolar sorting: not so different after all! Biochem Soc Trans *44*, 891–897.

Magalhães, RSS, Popova, B, Braus, GH, Outeiro, TF, and Eleutherio, ECA. (2018). The trehalose protective mechanism during thermal stress in Saccharomyces cerevisiae: the roles of Ath1 and Agt1. FEMS Yeast Res. *18*, foy066.

Mai, C.T., Le, Q.G., Ishiwata-Kimata, Y., Takagi, H., Kohno, K., and Kimata, Y. (2018). 4-Phenylbutyrate suppresses the unfolded protein response without restoring protein folding in Saccharomyces cerevisiae. FEMS Yeast Res *18*.

Merksamer, P.I., Trusina, A., and Papa, F.R. (2008). Real-time redox measurements during endoplasmic reticulum stress reveal interlinked protein folding functions. Cell *135*, 933–947.

Miyagawa, K.-I., Ishiwata-Kimata, Y., Kohno, K., and Kimata, Y. (2014). Ethanol stress impairs protein folding in the endoplasmic reticulum and activates Ire1 in Saccharomyces cerevisiae. Biosci Biotechnol Biochem *78*, 1389–1391.

Mori, K. (2009). Signalling pathways in the unfolded protein response: development from yeast to mammals. J. Biochem. *146*, 743–750.

Mori, K., Ma, W., Gething, M.J., and Sambrook, J. (1993). A transmembrane protein with a cdc2+/CDC28-related kinase activity is required for signaling from the ER to the nucleus. Cell *74*, 743–756.

Mori, K., Kawahara, T., Yoshida, H., Yanagi, H., and Yura, T. (1996). Signalling from endoplasmic reticulum to nucleus: transcription factor with a basic-leucine zipper motif is required for the unfolded protein-response pathway. Genes Cells *1*, 803–817.

Ozcan, U., Yilmaz, E., Ozcan, L., Furuhashi, M., Vaillancourt, E., Smith, R.O., Görgün, C.Z., and Hotamisligil, G.S. (2006). Chemical chaperones reduce ER stress and restore glucose homeostasis in a mouse model of type 2 diabetes. Science *313*, 1137–1140.

Promlek, T., Ishiwata-Kimata, Y., Shido, M., Sakuramoto, M., Kohno, K., and Kimata, Y. (2011). Membrane aberrancy and unfolded proteins activate the endoplasmic reticulum stress sensor Ire1 in different ways. Mol Biol Cell *22*, 3520–3532.

Ranga Rao, S., Subbarayan, R., Ajitkumar, S., and Murugan Girija, D. (2018). 4PBA strongly attenuates endoplasmic reticulum stress, fibrosis, and mitochondrial apoptosis markers in cyclosporine treated human gingival fibroblasts. J Cell Physiol *233*, 60–66.

Rao, R., Nakamoto, R., Verjovski-Almeida, S., and Slayman, C.W. (1992). Structure and function of the yeast plasma-membrane H+-ATPasea. Annals of the New York Academy of Sciences *671*, 195–203.

Riordan, J.R. (1999). Cystic fibrosis as a disease of misprocessing of the cystic fibrosis transmembrane conductance regulator glycoprotein. Am J Hum Genet *64*, 1499–1504.

Ron, D., and Walter, P. (2007). Signal integration in the endoplasmic reticulum unfolded protein response. Nat. Rev. Mol. Cell Biol. *8*, 519–529.

Shamu, C.E., and Walter, P. (1996). Oligomerization and phosphorylation of the Ire1p kinase during intracellular signaling from the endoplasmic reticulum to the nucleus. EMBO J *15*, 3028–3039.

Sheppard, D.N., and Welsh, M.J. (1999). Structure and function of the CFTR chloride channel. Physiological Reviews *79*, S23–S45.

Sikorski, R.S., and Hieter, P. (1989). A system of shuttle vectors and yeast host strains designed for efficient manipulation of DNA in Saccharomyces cerevisiae. Genetics *122*, 19–27.

Tanaka, K. (2009). The proteasome: Overview of structure and functions. Proc Jpn Acad Ser B Phys Biol Sci *85*, 12–36.

Tapia, H, Young, L, Fox, D, Bertozzi, CR, and Koshland, D. (2015). Increasing intracellular trehalose is sufficient to confer desiccation tolerance to Saccharomyces cerevisiae. Proc Natl Acad Sci USA. *112*, 6122-6127.

Thibaudeau, T.A., and Smith, D.M. (2019). A Practical review of proteasome pharmacology. Pharmacol Rev *71*, 170–197.

Toyoshima, C., Nakasako, M., Nomura, H., and Ogawa, H. (2000). Crystal structure of the calcium pump of sarcoplasmic reticulum at 2.6 Å resolution. Nature *405*, 647–655.

Umebayashi, K., Hirata, A., Fukuda, R., Horiuchi, H., Ohta, A., and Takagi, M. (1997). Accumulation of misfolded protein aggregates leads to the formation of russell body-like dilated endoplasmic reticulum in yeast. Yeast *13*, 1009–1020.

Valetti, C., Grossi, C.E., Milstein, C., and Sitia, R. (1991). Russell bodies: a general response of secretory cells to synthesis of a mutant immunoglobulin which can neither exit from, nor be degraded in, the endoplasmic reticulum. J Cell Biol *115*, 983–994.

Winston, F., Dollard, C., and Ricupero-Hovasse, S.L. (1995). Construction of a set of convenient Saccharomyces cerevisiae strains that are isogenic to S288C. Yeast *11*, 53–55.

Zattas, D., and Hochstrasser, M. (2015). Ubiquitin-dependent Protein Degradation at the Yeast Endoplasmic Reticulum and Nuclear Envelope. Crit Rev Biochem Mol Biol *50*, 1–17.